Chitosan-based smart hybrid materials: a physico-chemical perspective

Giuseppe Cavallaro, Samantha Micciulla, Leonardo Chiappisi, Giuseppe Lazzara

Journal Name

ARTICLE TYPE

Cite this: DOI: 00.0000/xxxxxxxxxx

Chitosan-based smart hybrid materials: a physico-chemical perspective

Giuseppe Cavallaro,[a] Samantha Micciulla,*[b], Leonardo Chiappisi*[b] and Giuseppe Lazzara*[a]

Received Date
Accepted Date

DOI: 00.0000/xxxxxxxxxx

Chitosan is one of the most studied cationic polysaccharides. Due to its unique characteristics of being water soluble, biocompatible, biodegradable, and non-toxic, this macromolecule is highly attractive for a broad range of applications. In addition, its complex behavior and the number of ways it interacts with the different components in the system results in an astonishing variety of chitosan-based materials. Herein, we present recent advances in the field of chitosan-based materials from a physico-chemical perspective, with focus on aqueous mixtures with oppositely charged colloids, chitosan-based thin films, and nanocomposite systems. In this review, we focus our attention on the physico-chemical properties of the chitosan-based materials, including solubility, mechanical resistance, barrier properties, and thermal behaviour, and provide a link to the chemical peculiarities of chitosan, such as its intrinsic low solubility, high rigidity, large charge separation, strong tendency to form intra- and inter-molecular hydrogen bonds, etc..

Introduction

Chitosan is commonly obtained from the deacetylation of chitin, the second abundant natural polymer on earth after cellulose[1]. The primary sources of chitin are crustaceans such as crabs, shrimp and lobsters, which are highly abundant waste products from the food, beverage and canning industries[2,3]. The backbone of chitosan is very similar to cellulose, with the hydroxyl group on the C2 position replaced either by an amino or acetylamino group. Thus, chitosan is a copolymer consisting of N-acetyl-2-amino-2-deoxy-d-glucopyranose and 2-amino-2-deoxy-d-glucopyranose, where the two types of repeating units are linked by (1→4)-β-glycosidic bonds. The chemical structure of chitosan is shown in Fig. 1a. It is available within a large range of molecular weight and degree of deacetylation. These two parameters largely alter the physico-chemical properties of the biopolymer and therefore a variety of specific applications can be considered based on viscosity, biological activity, biodegradability, wettability, colloidal stability and pH responsive features. Chitosan is readily soluble in dilute acidic solutions below pH 6.0 due to the protonation of the amine groups (pKa value of 6.3). Furthermore, it has gel, fibers and film forming properties. From the biological point of view it shows antimicrobial activity, and good compatibility with living tissue.

Chitosan exhibits a combination of physico-chemical features which make this polymer a fundamental component in material science. With the exception of cationically modified cellulose, it is one of the very few cationic biopolymers available. The saccharidic backbone provides this macromolecule with three fundamental peculiarities, not found in other polymers: *(i) A high intrinsic rigidity*, with reports of persistence lengths which vary between 5 and 30 nm[4,5]. *(ii) a relative large spacing between the charges*, with a maximum of 1 charge per 5 Å in the case of fully deacetylated polymer. The actual value is in reality much closer to the Bjerrum length in water of 7.1 Å, i.e., the distance at which the magnitude between electrostatic interaction approaches the thermal energy. The consequence of the large separation, in combination with the high intrinsic rigidity, is the fact the polymer conformation in solution is less affected by the type and concentration of counterions or by the binding to oppositely charged colloids compared to high charge density, flexible, polymers. *(iii) A high tendency of forming intra- and inter-molecular hydrogen bonds*. Such hydrogen bonds increase, on the one side, the rigidity of the polymer backbone, and are, on the other side, at the origin of the very low tendency of mixing between polysaccharides and other polymers.

Chitosan-based materials have been reviewed in different fields, from molecular separation to food packaging film, from artificial skin to bone substitutes and water treatment[3,3,6,7]. Most of the reviews are focused on a given application of the chitosan-based materials[6–10] or in some other cases they explore a wide range of biopolymers, including chitosan, for some specific applications[11]. How these and further peculiarities affect the properties of soft, chitosan hybrid compounds in aqueous environment, in thin films, and in nanocomposite systems, schematically represented in Figs. 1b-d, is discussed hereafter.

[a] *Dipartimento di Fisica e Chimica, Università degli Studi di Palermo, Viale delle Scienze pad 17, 90128 Palermo, Italy; E-mail: giuseppe.lazzara@unipa.it*
[b] *Institut Max von Laue - Paul Langevin, 71 avenue des Martyrs, 38042 Grenoble, France. E-mail: micciulla@ill.eu, chiappisil@ill.eu*

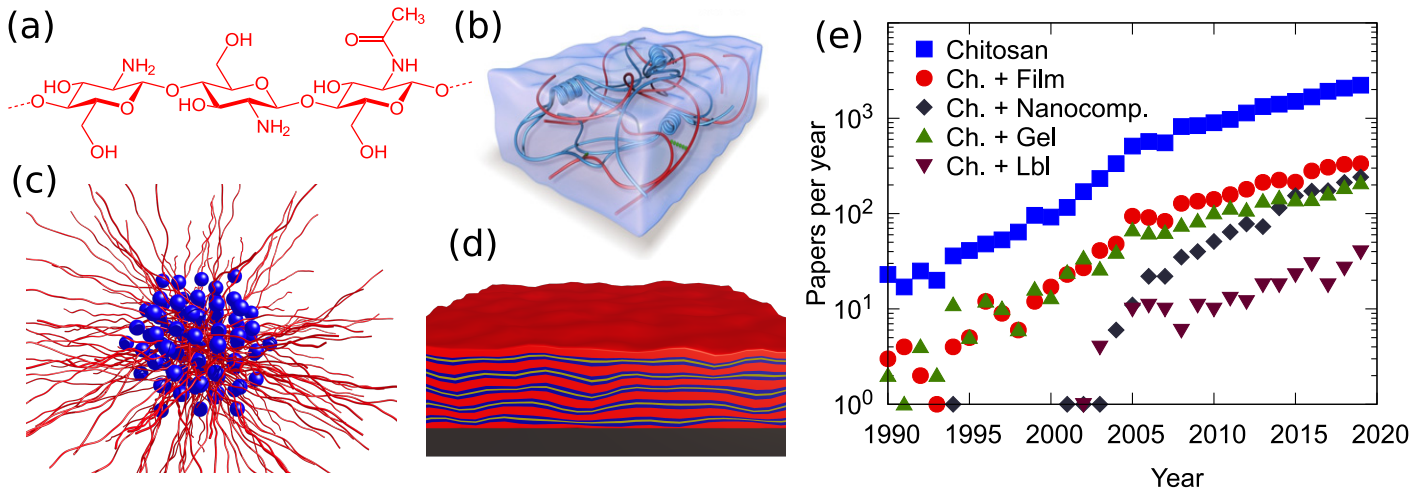

Fig. 1 (a) chemical structure of chitosan; and schematic representations of (b) of hybrid hydrogel, from Ref. 12; of (c) chitosan/surfactant complexes,(d) chitosan-based layered coatings and (e) number of publications per year on Chitosan based materials. Data are from Scopus and they were obtained on 1. June 2020 using as searching string TITLE-ABS-KEY ("Chitosan" and "material") or ("Chitosan" and "material" and "film"), ("Chitosan" and "material" and "gel"), ("Chitosan" and "material" and "LbL") or ("Chitosan" and "material" and "nanocomposite");.

It is also useful to recall that chitin, the precursor of chitosan and main structural component of the exoskeleton of crustaceans, is, by design, a very poorly soluble polymer. This intrinsic property is retained in chitosan, whose solubility in acidic aqueous environment is simply given by the translational entropy of the counterions. In other terms, as soon as the soluble counterions, often acetate ones, are exchanged with much less soluble, macroions such as polymers, micelles, or clay particles, the formation of an insoluble complex is observed. We find this general tendency trough out the physico-chemistry of chitosan-based systems, and, in the course of this review, we will highlight how this phenomenon is exploited and which strategies were developed to increase the solubility.

As illustrated in Figure 1e, chitosan is highly employed in material science. Film and gel formulations are the most traditional investigated materials, since 2005 nanocomposites have been growing. Until now less explored but promising, is the possibility to prepare Layer-by-Layer system using chitosan as cationic biopolymer. The observed trends suggest that although the applications of this polymer have been established, some properties, such as mechanical strength, thermal stability, low water content and gas barrier properties resulted not good enough to meet this wide range of applications. The preparation of hybrid materials based on chitosan, with both organic or inorganic fillers, overcome some intrinsic limitations and opportunely tune the physico/chemical properties of the material.

Soft materials in aqueous media

The above mentioned properties of chitosan make this polymer a unique building block in the field of colloidal chemistry. Accordingly, substantial efforts have been given to characterize chitosan hydrogels, or complex mixtures of chitosan with surfactants, polymers, emulsions, etc.

Chitosan/Surfactant systems

Mixtures of chitosan and surfactants have been a matter of intensive studies[13–15]. Given its cationic nature, particular attention has been dedicated to mixtures of chitosan with oppositely charged anionic surfactant. It can be safely stated that chitosan forms insoluble complexes with strongly ionic surfactants over a wide range of concentration and mixing ratios[13,16–18], with the formation of insoluble complexes even at very low surfactant concentration (mM) and large polymer excess[15]. A clear explanation of this extremely pronounced low solubility has not been found, yet, and the experimental results point towards a kinetically trapped state and highly cooperative binding. The high tendency to form water-insoluble complexes has been exploited for the preparation of beads[13,19], whose size can be controlled by the preparation method and varies between few hundred nanometers and few centimeters. The thickness of the bead wall shows an initial growth with the square root of time, indicating a diffusion controlled process[13]. Such beads are highly promising for pollutant recovery applications[19,20].

Few studies have been focused on the interaction of chitosan with fatty acids[21–24]. Due to the fact that chitosan is soluble in slightly acidic medium, while long and medium chain fatty acids are solubilized in alkaline condition, soluble mixtures are found only when chitosan is mixed with short chain carboxylic acids, such as formic, acetic, butyric and valeric acid[21,25]. Due to the short alkyl chain, the interactions in these systems are purely electrostatic[21]. As soon as the alkyl chain is long enough, lateral, hydrophobic interactions favors the spontaneous formation of micelles, and a much more complex behavior in mixtures with chitosan is observed. This is the case, for instance, of mixtures with undecylenic acid, which exhibit the formation of supramolecular aggregates with a typical size of few hundred nanometers[26]. Mixtures of chitosan with long chain acids, such as oleic, linoleic, palmitic, and stearic acid, have also been studied[22,27], despite their low solubility, as mentioned before. A schematic represen-

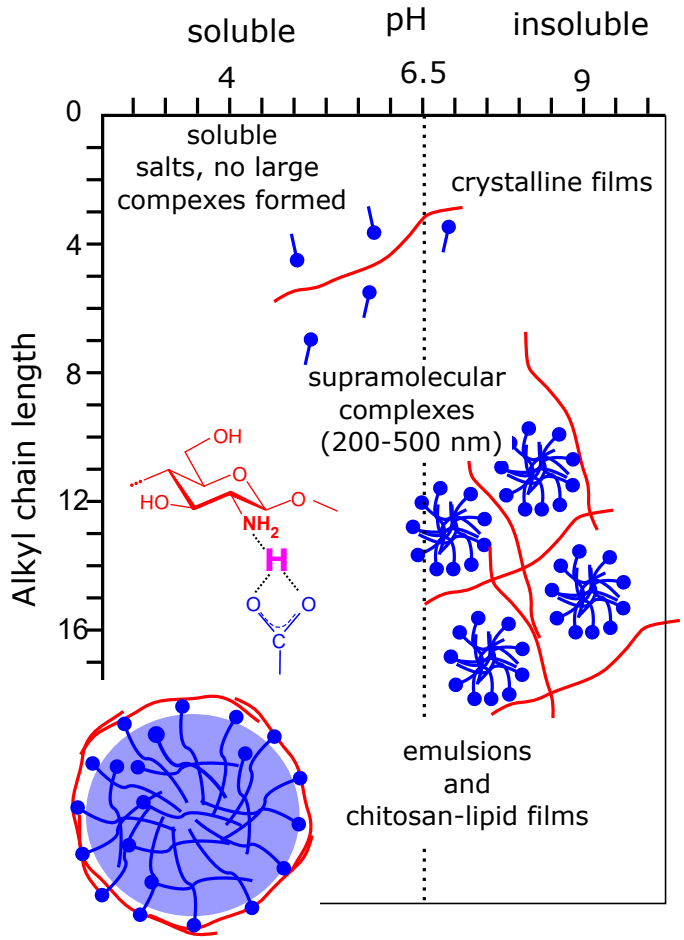

Fig. 2 Schematic representation of structures and interaction mechanism found in chitosan/carboxylic acids as a function of the acidity of the solution and of the length of the alkyl chain. Insets represent the structures observed in the mixtures and a insight into the ionic hydrogen bond formed between the carboxylic acid termination and the amine moiety of chitosan. Adapted with permission from Ref. 15

tation of the structures formed in carboxylic acid/chitosan mixed systems is provided in Fig. 2. However, water soluble complexes can be obtained when chitosan oligosaccharides, which as soluble also in alkaline conditions, are used. An example are mixtures of chitosan oligosaccharide with oleic acid vesicles[28,29]. The coating by chitosan decreased the fluidity of the membrane and increased the stability of the liposomes towards shear and flow stresses[28].

The strong limitation found for the incompatible difference in solubilities of chitosan and fatty acids is overcome when the fatty acids are chemically modified to include an oligoethylene oxide block between the aliphatic chain and the carboxylic acid termination. So called alkyl ether carboxylates were shown to co-assemble with chitosan in a broad variety of structures which are highly responsive to external stimuli[30–34]. In particular, depending on the solution acidity and the molecular architecture of the surfactant, multilayer vesicles or compact aggregates embedding small surfactant micelles are obtained[14,31,34]. To the best of our knowledge, these surfactant/chitosan systems are those showing the largest structural variety with an exquisite response to pH variations. The large structural variety derives from the high control over the surfactant packing parameter, depending on pH and on the ratio between alkyl chain and size of the oligo ethylene oxide block. The strong response to even very little changes in solution acidity derive from the very specific ionic hydrogen bond between the carboxylic surfactant termination and the amine moiety of the macromolecule with an estimated strength of 10 k_BT[32,35]. In contrast to generic electrostatic interactions, the ionic hydrogen bridges are extremely localized and their strength strongly dependent on pH. The peculiarity of this bond is probably also at the origin of the very unique observation of chitosan-fatty acid mixtures becoming less soluble upon addition of a nonionic surfactant[32]. Finally, the strong structural response of these systems towards mild variations in pH can be exploited for the formulation of environmentally friendly delivery and recovery systems[34].

Chitosan-based polyelectrolyte complexes

The formation of supramolecular complexes in mixtures with anionic polyelectrolytes has been extensively studied, and we address the readers to some extensive reviews[36,37]. As indicated in the introduction, chitosan is an intrinsically insoluble polymer, and its solubility is provided by the counterion cloud. In mixtures with oppositely charged polyelectrolytes, these many, soluble counterions are exchanged with an ionic macroion. Accordingly, the most common finding is that an insoluble coacervate is formed. This condition has motivated the establishment of various strategies to prepare more water-soluble systems, such as dispersed colloidal complexes or hydrogels. The formation of complexes can also be exploited for the formation of thin films, which are discussed in the next section of this review. A schematic description of the different typologies of chitosan-based polyelectrolyte complexes is given in Fig. 3.

Mixtures of chitosan with virtually every other available polyanion were investigated. However, particular attention has been put on complexes with polynucleutides, such as DNA[38–42] or RNA[43–46], with anionic polysaccharides, such as alginate[9,47–50], hyaluronic acid[51,52], dextran sulfate[53,54], or synthetic polyelectrolytes, such as poly Acrylic Acid[55–58].

The main objective of studying chitosan-polynucleotides mixtures is the understanding and improvement of gene delivery systems[59,60]. In this sense, it is essential to determine the factors affecting the affinity between chitosan and the polynucleotide, in order to be able to balance the stability of the complexes and the delivery efficiency. A complex with a too high binding constant cannot release the gene to the target cell. In contrast, a complex with a too low affinity is not able to transport the gene sequence to the target cell. In this sense, isothermal titration calorimetry provides valuable insights into the binding affinity of chitosan and DNA or RNA[40,42,46]. The binding is mainly due to the electrostatic interaction between the charged amine group of the polysaccharide and the phosphate unit of the nucleic base[41,42], and is therefore affected by the degree of acetalytion and the degree of ionization of chitosan.

Given the biocompatible properties of anionic polysaccharides, such as alginate and hyaluronate, their exomplexes with chi-

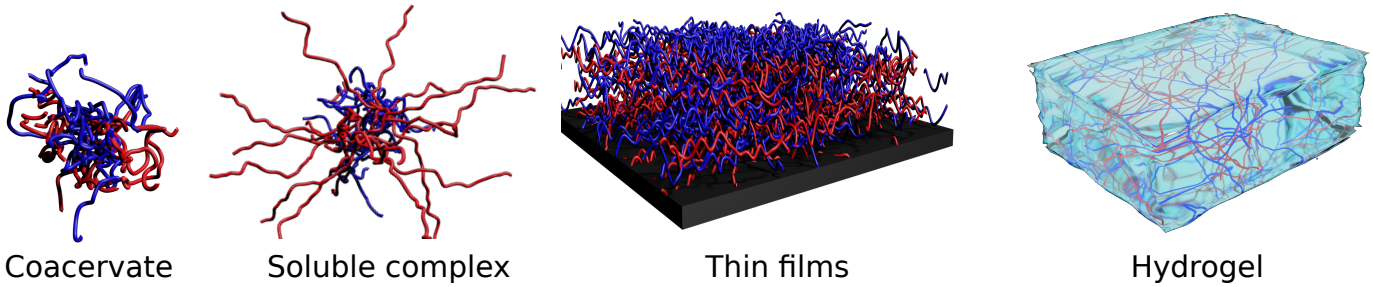

Fig. 3 Schematic representation of (a) complex coacervates, (b) soluble complexes, (c) solid supported thin films, and (d) gellified systems obtained from mixtures of chitosan (in red) and oppositely charged polyanions (in blue)

.

tosan have been extensively investigated, mainly as scaffolds for tissue engineering[37,47,48], for drug delivery[47,49], or for pollutant recovery[9,50], to mention some of the most relevant applications. The properties of chitosan/alginate scaffolds can be further improved when a third component is added to the mixture, such as inorganic nanoparticles[61–63], or by chemical cross-linking agents[64,65]. Similarly, chitosan/hyaluronic acid complexes are highly interesting in tissue engineering applications due to the combined flexible nature and antibacterial properties of such complexes. In particular, hydrogels can be formed *in situ* upon injection to the desired tissue, due to the slow kinetics of gel formation[66]. When chitosan is mixed with dextran sulfate, a strongly charged polyion, the formation of capsules and beads is observed even in large excess of one of the components[53,54,67], similarly as for mixtures of chitosan with sulfated surfactants described earlier.

Poly(acrylic acid) (PAA) is one of the most relevant synthetic weakly anionic polymers and complexes with chitosan were probed, mainly with the aim of designing pH-responsive delivery systems. The preparation of chitosan/PAA complexes follows two main routes: non-crossed linked particles are prepared by mixing chitosan and PAA in different stoichiometries and experimental conditions[55,56]; cross-linked chitosan PAA particles are obtained when acrylic acid is polymerized in the presence of chitosan[57].

Chitosan-based hydrogels

The challenge of preparing chitosan-based hydrogels lies in the fact that a significant amount of water needs to be retained in the system. Chitosan hydrogels are generally prepared by physical or chemical cross-linking of the polymer chains, keeping enough charges and/or hydrophilic moieties to guarantee sufficient hydration in the network. There are numerous protocols for the preparation of simple and hybrid chitosan hydrogels, which are attracting large interest, in particular in the fields of biomedical applications[12,68,69] and wastewater treatment[70].

Physically cross-linked simple hydrogels Chitosan-based hydrogels are formed by physical or chemical cross-link between the polymer chains. The simplest procedure consists in increasing the pH of the chitosan solution, thus strongly reducing the solubility of the polymer[71,72]. In practice, a concentrated solution of chitosan is brought into contact with an alkaline environment. The swelling of these precipitate/hydrogel is determined by the osmotic pressure of the counterions of the residual charges on the chitosan backbone. In particular, Enache *et al.* showed that the advancement of the gelation front can be adequately described with Fick's second law[72]. Moreover, different studies have reported that the chitosan hydrogel structure becomes more heterogeneous the larger the distance from the hydrogel surface[71,72].

A different approach consists in using multivalent, negative ions to physically cross-link chitosan via electrostatic interactions. While tripolyphosphate is the most common anionic cross-linking agent[73–76], examples of ionotropic gelation of chitosan by molybdate[77], polyoxometalates[78], sulfate[79], citrate[79], or phytate[12] have been also reported. A clear advantage of using tripolysphosphate as cross-linking agent is the high mechanical stability of the obtained particles. For instance, it was shown that the mechanical strength of chitosan/tripolyphosphate gel beads are approximately ten times higher than the analogous beads prepared by cross-linking the polymer with sulfate and citrate[79]. Noteworthy, the system chitosan/β-glycerophosphate shows a thermal induced gelation when the system is heated at 37 °C, thus being ideally suited for the preparation of injectable chitosan hydrogels[80,81]. A further interesting example is the formation of a hybrid chitosan-gelatin hydrogel, whose mechanical properties are strongly enhanced upon addition of phytate, a multivalent negatively charged ion, to the hydrogel[12] (as depicted in Fig. 4). This system provides an excellent example on how the physicochemical properties of chitosan are linked to the hydrogel features. In fact, when chitosan is neutralized with sodium phytate, a rather dense precipitate is formed, due to the high charge density and stiffness of the polysaccharide. In contrast, a well hydrated, elastic hydrogel is formed when chitosan is co-crosslinked with a flexible, hydrophilic, and loosely charged polymer such as gelatin. Finally, an important property found in chitosan hydrogels formed by ionic cross-link with anionic polysaccharides is the self-healing capacity of these gels, which originates from the dynamic nature of the ionic cross-linking point[61,82].

Chemically cross-linked simple hydrogels Covalent cross-link of chitosan is also performed in a routine fashion. In many cases, small molecules such as dialdehydes[83,84] or Genipin[85,86] are used. To improve the elasticity of the gel, polymeric cross-linking agents such as diepoxy polyethylene glycole or dicarboxylic acid polyethylene glycole are also employed[87,88].

Hybrid hydrogels To add new functionalities and to adapt

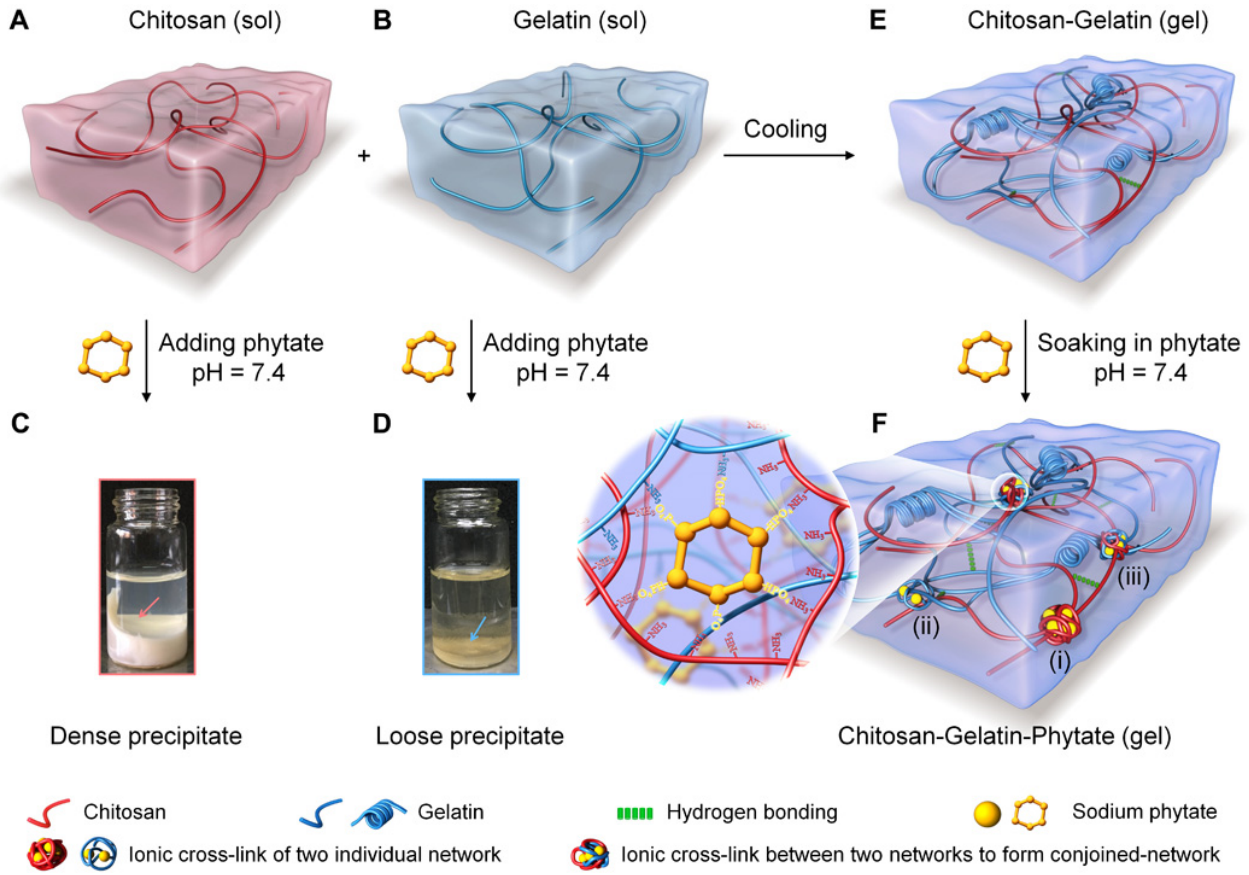

Fig. 4 Schematic representation of chitosan (A) and gelatin (B) solutions which form a composite hydrogel upon mixing and cooling (E). Optical photos of the dense precipitate formed by chitosan (C) and of the the loose precipitate formed by gelatin (D) upon addition of sodium phytate. The different degree of hydration of the precipitate is the direct consequence of the different charge density and stiffness of chitosan and gelatin (F) Schematic representation of the chitosan, gelatin, phytate conjoined-network hydrogel. Inset illustrates the structure of the network, consisting of physical bridging between the polymer chains cross-linked by the multivalent counterion. The cross-bridging of the two networks allows to obtain a unique combination of high compressive modulus and toughness. Reprinted with permission from Ref. 12.

the mechanical properties of the hydrogels to the desired needs, the formation of hybrid chitosan-based hydrogels has been extensively probed. The strong adhesive, antiinflammatory, hemostatic, and bactericidal properties of chitosan make this polysaccharide an excellent candidate for a broad range of biomedical applications of hydrogels. We address the reader to some recent reviews on the topic[6,68,69].

We have mentioned above the formation of hydrogels based on chitosan and hyaluronic acid for biomedical purposes[52,66,89]. To provide mechanical stability to these hydrogels, a covalent cross-link between the two polysaccharides can be obtained via a Schiff's base reaction. Chemical pre-functionalisation of chitosan with a N-succinyl group and of hyaluronic acid with an aldehyde one, allows the reaction to occur *in situ* without the need for additional chemicals[89]. Similar cross-link procedures are applied to other polysaccharide based hybrid hydrogels[90,91]. A plethora of different chemical modifications of chitosan to enable the chemical cross-link within chitosan/polysaccharide networks is described in literature[92,93] and the right choice must be dictated by the field of application, the nature of the components, and the desired physical properties of the resulting hydrogel. Noteworthy are externally-triggered cross-link reactions, e.g., by photoirradiation[94,95].

In summary, extensive work has been performed on the characterization of chitosan-based hydrogels and the understanding of the correlation between molecular properties (degree of substitution, charge density, complex solubility, and the final gel characteristics. In particular, their use in the field of tissue engineering seems to be highly promising, given the 3D network structure of the gel, the tunable mechanical properties, associated with the strongly adhesive, anti-inflammatory, and anti-bacterial properties of chitosan.

Self-assembly of chitosan-based thin films

Besides hydrogels, polysaccharide assemblies in the form of thin films are very well suited for the design of functional coatings dedicated to biomedical and biotechnological purposes[96–100]. Among them, chitosan-based thin films have been widely applied for drug delivery systems[101–103], antibacterial[104–107], and antifungal surfaces[103,108,109], food protection and paper packaging[110,111], as well as for wound healing[112,113]. The broad range of applications is possible thanks to the excellent biocompatibilty,

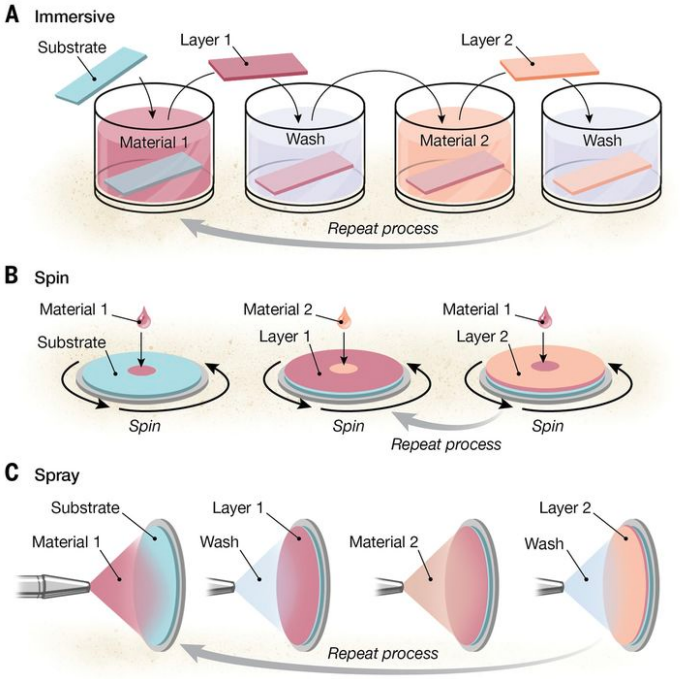

Fig. 5 Schematic illustration of different methods for the LbL assembly process: (a) dipping method, (b) consecutive spin-coating, and (c) spraying of oppositely charged polyelectrolytes. Image adapted from Ref. 114.

biodegradibility, low toxicity and high availability of chitosan, as well as to the tunable film properties (structure, elasticity, porosity) by adjusting both molecular composition and assemblies conditions [13].

One of the most commonly employed strategies for the formation of chitosan-based thin films, is to exploit the ionic character of the polysaccharide to form polyelectrolyte multilayers (PEMs) [103,114–116]. The simplest preparation approach consists in the alternate adsorption of oppositely charged species onto a charged substrate, known as layer-by-layer (LbL) deposition [117] (see Figure 5a). The main driving force for the complexation of oppositely charged macromolecules is the entropic gain associated to counterions release [118], a universal prerequisite for both synthetic and natural colloidal species.

The ease of preparation and extreme versatility of the method comes with a remarkably fine control of the film properties, such as thickness, roughness, internal layer structure, elasticity, porosity by selecting materials, solvent quality, pH, ionic strength [119,120].

Among the most popular combinations of chitosan with natural polyelectrolytes, we find alginate [121–124] and hyaluronic acid [103,107,125]. Alginate has the ability to form gels by ion bridges in the presence of multivalent cations, e.g., calcium, due to the presence of carboxyl groups along the polymer backbone. Due to the porous structure and high water-absorption capacity of alginate-based assemblies, it is a promising and largely employed material for the design of wound dressings [126]. Concerning hyaluronic acid, it is almost ubiquitous in the human body and serves as an essential component mediating cellular signaling, wound repair, morphogenesis and matrix organization [127]. Furthermore, it is popular for its high flexibility, which becomes more relevant with increasing molecular weight. [128] Multilayers prepared from its combination with chitosan, which is known to participate to up-regulation of genes related to calcium binding and mineralization promoting bone formation [129], have been proposed as potential "generic" surface treatment, since simple variation of scaffold morphology, protein attachment and additives incorporation render such films suitable for most tissue engineering applications [113]. Interestingly, the properties of the individual polyelectrolytes are partially retained in their surface properties, as evidenced by the surface hydrophilicity measured by water contact angle [107] (Figure 7g), and it represents a convenient way to monitor the subsequent layer adsorption. A water contact angle between 80 and 100° is most commonly reported for chitosan-terminated PEMs, while the value decreases to 40-50° for alginate or hyaluronic acid termination.

Similar to synthetic weak polyelectrolytes [130,131], the properties of both chitosan/alginate and chitosan/hyaluronic acid pairs are pH dependent, which allows tuning the properties of the resulting films. In particular, thicker and rougher layers can be formed at pH between 3 and 5 [122], where the charge mismatch between low charge density chitosan and high charge density alginate (or hyaluronic acid) chains leads to the adsorption in a more coiled conformation. Such charge mismatch induces also larger mass adsorption to achieve charge neutralization [132]. The increment of surface roughness when chitosan/hyaluronan multilayers are used to coat solid substrates is very advantageous for cell adhesion, proliferation and differentiation, making them excellent bone scaffolds [133]. Regardless of the pH, the increase of ionic strength always results in the formation of thicker layers due to a stronger extrinsic charge compensation [124,134,135] and, analogous to synthetic polymers, ionic strengths below 10^{-4} mol/L prevents layer growth [136].

The ensemble of characteristics of a deposition protocol, namely polymer molecular weight and architecture, ionic strength and type of ions, pH, temperature, always defines the growth mechanism and the final properties of the multilayer, with the growth mechanism being an indication of the interaction strength within complexes. The low charge density, a consequence of the large intrinsic persistence length characteristic of chitosan, is the reason for the non-linear growth regime observed during the LbL deposition of several chitosan-based PEMs [106,132]. When the chitosan chains are loosely bound, they diffuse within the film, which enhances the mass uptake per adsorption cycle. The growth mechanism is therefore governed by the ability of chitosan of diffusing through the pre-adsorbed layers (in/out model) [137], with high MW chains diffusing less than their low MW equivalents [132]. A convenient way to highlight this two-step layer growth (adsorption and diffusion) is by monitoring the polyelectrolyte adsorption *in-situ* by the quartz crystal microbalance with dissipation monitoring (QCM-D) (Figure 7e). The working principle of the technique exploits the piezoelectric properties of a quartz crystal under the application of an oscillating shear stress. The freely decaying damped sinusoidal oscillation of the crystal measured between subsequently applied

shear deformations is registered and analysed with respect to the oscillation of an unload crystal. As a result of the mass coupled to the surface, the oscillation frequency f decreases, while the speed of the amplitude decay can be interpreted as a measure of the energy dissipated by the system coupled to the surface, *i.e.* the film viscoelasticity. The oscillation of the sensed mass has been a valid parameter to identify a typical behavior of highly diffusive polymers, which give very large mass uptake upon each adsorption steps. This is the case of chitosan in combination with both alginate and hyaluronan, whose layer growth can show a characteristic *odd-even* effect[113,138]. In addition to the diffusion through the film, such a behavior can be also explained by the pronounced hydration of chitosan layers, responsible for higher mass uptake (hydration water) and the pronounced layers swelling[115,122], therefore well identifiable from the frequency shift/dissipation change upon layer formation and in combination with measurements of the "dry" mass by ellipsometry (Figure7a). Differently from chitosan, high charge density polymers, like poly-L-lysine, lead to denser sequence of interaction sites per chain and stronger PE-PE complexation at first contact[124], like the case of Alginate/poly lysine complexes forming very compact PEMs.

Besides the association with biopolymers, fundamental studies of chitosan with synthetic polymers, for instance poly(acrylic acid), have been particularly useful[139,140]. One of these studies have highlighted another mechanism leading to the exponential growth: the formation of islands by the first deposited layers, which growth laterally and vertically with the number of deposition cycles[120,137].

A fundamental aspect for (bio)technological applications of functional coatings is their stability to physiological and harsh conditions. For chitosan-based thin films, it has been observed that post-preparation stabilization *via* cross-linking is valuable tool to enhance their mechanical and chemical stability under both acidic and alkaline conditions[141,142]. In addition to providing mechanical stability, cross-linking seems to control the extent of protein adsorption onto the modified substrate[113,143]. This possibility is not offered by all polymers, ans it renders chitosan particularly interesting for post-synthetic modifications. Particularly relevant for regenerative tissue engineering and as antimicrobial surfaces[144] are those functional coatings combining chitosan with pectin. In this case, the 1:1 charge ratio achieved at pH 5.6 suppress the chitosan diffusion and reduces its water uptake, which results ina linear thickness increment with initial mass uptake attachment and a slower chain rearrangement[135]. An important prerequisite for the film stability is that both polyelectrolytes are charged, and this corresponds to pH between 3.6 and 7, and salt concentration between 0.05 and 0.15 M NaCl[145].

Another very promising system for regenerative medicine is represented by chitosan/collagen films. Collagen is a fibrous protein that plays an important role in tissue healing, providing a suitable biological environment for cell growth and attachment, migration, and proliferation[146]. Thin film of collagen and low or high MW chitosans showed enhanced tensile strength and elongation at break compared to a pure collagen films, as the intermolecular interactions within the matrix mitigate the strong intramolecular interaction within collagen chains, which increases the film flexibility[147]. Furthermore, chitosan contributes to preserve the native structure of collagene, limit hydrolitic and enzymatic degradation, and reduce the swelling of collagen film (efficient moisture barrier), which could allow a controlled release of epidermal growth factors, when films are used as wound dressings[147,148].

Among the rich variety of combinations of chitosan and other polysaccharides in thin films for biomedicine and biotechnology, it is worth to mention the use of silk[149], casein[150], fucoidan[112], cellulose[151], and DNA[152]. In some cases, highly cross-linked structures, as confirmed by surface chemical characterization by X-ray photoelectron spectroscopy, are formed by reactive side grous. Furthermore, enhanced biofilm stability, like mucin, against degradation in surfactant solutions has been proven in presence of chitosan, as the interactions with the polysaccharide reduce the hydrophobic interactions with the surfactant molecules and preserves the binding to the solid substrates[153]. Finally, the possibility of driving the assembly of inorganic nanoparticles (NPs), e.g. gold (Au)-NPs[154], for the preparation of surface electrodes and impedance spectroscopy studies has been also reported, which is added to the numerous examples of highly relevant applications of chitosan-based thin films for the design of bioengineering surfaces, among which antimicrobial surface[103,104,155] and modulated drug release[103], for biosensoring[156], anticancer treatment[157], anticoagulant for implants in cardiovascular surgery[158], food preservation[111,159], lubrication[100], release of fertilizers[160], and flame retardant[108].

For most of these applications, simple preparation methods, simple to speed and scale up for industrial purposes, are fundamental, therefore alternate or simultaneous spin-coating or spraying of polyelectrolyte solutions[161] are valid alternatives to the LbL deposition (Figure 5b and 5c). Spraying polyelectrolyte solutions onto a substrate leads to similar structures as dipped multilayers, with minor differences in the growth kinetics of the very first layers due to the suppression of diffusive events[162,163] which results in thinner and smoother layers, as revealed by atomic force and fluorescence microscopy of synthetic polyelectrolytes[164,165], and it has been successfully applied to prepare chitosan-based multilayers onto flat[101,166] or curved surfaces[160]. Shape and dimension of chitosan:polyanion complexes remain crucial parameters for the film buildup by either alternate or simultaneous spraying, and they can be properly tuned by the mixing ratio and physico-chemical bulk properties.

The peculiarity of charge inversion from the cationic to the anionic form by proper chemical derivation has awarded the possibility of self-assemblying "one component" multilayers, fully based on chitosan.[167] The resulting thin films were very smooth and characterized by a linear layer increment, , due to the equal charge density along the chain for between polyanionic and polycationic form. Interestingly, their complexation was more exothermic (lower ΔH_{mix}) and more entropically favored (higher ΔS_{mix}) than for other chitosan/synthetic PE pair, resulting in an overall enhanced film stability.

Less popular than the LbL deposition, another method for thin

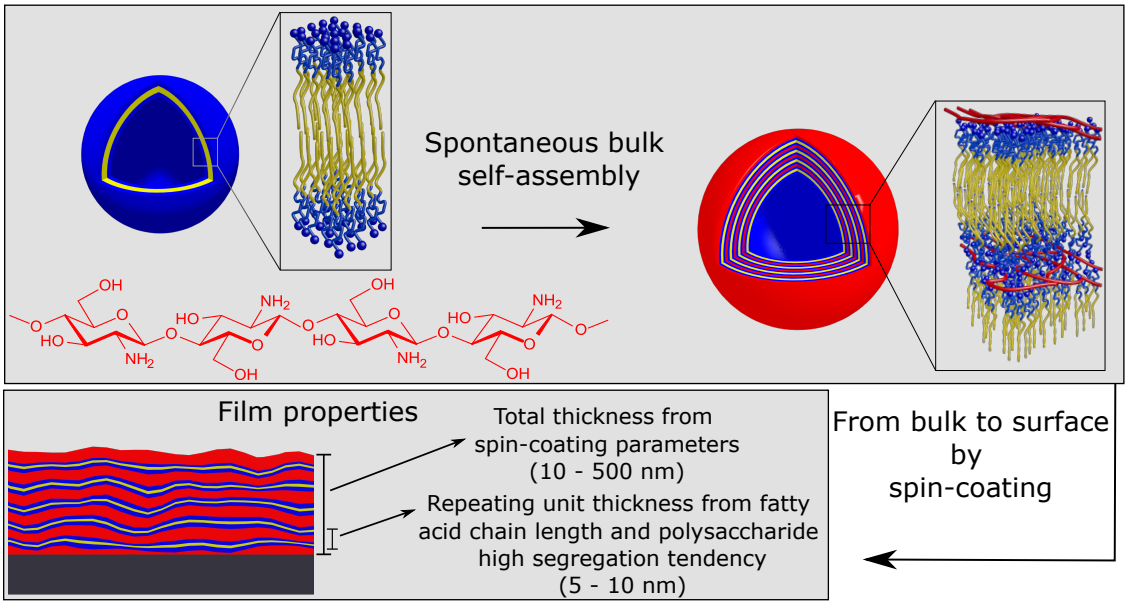

Fig. 6 Schematic representation of the formation of chitosan/fatty acid multilayered thin films via a one-step procedure which exploits the spontaneous association of the components into multilayered vesicles in solution. Adapted with permission from Ref. 33.

film preparation is the Langmuir-Blodgett technique. In this case, a Langmuir monolayer is formed by spreading an amphiphilic (macro)molecule dissolved in a volatile organic solvent on the surface of an aqueous subphase[168]. The molecules orient their hydrophilic part in the aqueous subphase and the hydrophobic moiety towards the hydrophobic phase (air), respectively. Such a monolayer is then transferred onto a solid substrate by the Langmuir– Blodgett (LB) process[169] by immersing (or emerging) a solid support in (or from) the aqueous subphase to recover the monolayer, with the possible formation of multilayers by multiple dipping iterations. LB multilayers have been prepared from amphiphilic chitosan derivatives, as well as their mixtures with phospholipids and cholesterol[170]. In this case, chemical modifications are a fundamental prerequisite to render chitosan soluble in organic solvents, and most frequently long alkyl chains are attached to the primary hydroxyl and amino group for this purpose[170,171].

The highly tunable structure of chitosan:fatty acid complexes in solution, forming multiwalled vesicles were prepared in bulk under tailored conditions (pH and mixing ratio) to obtain the desired dimension and number of layers[31], has been the key property for the development of a novel approach for the preparation of chitosan-surfactant multilayers from "one step" single step deposition[33]. This method overcomes the limitation of time consuming LbL assembly and offers more control on the internal layer structure than spraying methods. Chitosan:fatty acid complexes were then transferred onto a solid substrate by a single spin coating step, which spontaneously formed multilayers with high degree of inter-layer segregation. The control of structural key parameters, e.g. thickness and number of layers, from the bulk properties of the mixture ease significantly the preparation of films with tailored properties and functions. Furthermore, the low degree of intermixing between subsequent layers leading to high layer segregation makes this kind of multilayer suitable for selective release/uptake and exclusive response of individual parts to external stimuli. The highly segregated internal structure with individual water uptake of the hydrophilic moieties (chitosan layers) could be revealed only by exploiting the isotopic contrast of neutron reflectometry. In general, both X-ray and neutron reflectometry allow determining the internal volume fraction distribution of each component along the axis perpendicular to the surface. Their complementarity is due to the fact that theirs probes, photons and neutrons, interact with different subatomic element of an atom (the electron cloud and the nuclei, respectively), and therefore provide a different internal contrast of the same systems. In addition, neutrons interact differently with isotopes of the same nucleus, and this property can be as a tool for identifying internal structures of chemically homogeneous materials.

Our results showed that the morphology of coatings produced by this method is macroscopically highly homogeneous, but it phase-separates microscopically on a length scale of 5 nm. The electrostatic interaction between the amino-group of chitosan and the carboxilic termination of the fatty acids and the very low miscibility of chitosan with both hydrophilic and hydrophobic materials, is at the origin of the very small-scale segregation. Since the size of the microseparated domains depend on the degree of polymerization of the polymer and on the Flory–Huggins interaction parameter(s) χ with the different film components, a common strategy to prepare thin films with sub-10 nm structural features, essential for novel applications in nanolithography, is to use oligosaccharide based block-copolymers[172,173].

Finally, the preparation of chitosan thin films from end-tethering polymer chains onto solid surface, a geometry known as polymer brush[174,175], is worth to be mentioned. Either neutral or modified chitosan chains by quaternary ammonium salts, CHI-Q_x, were grafted to the epoxide derivatized silicon oxide

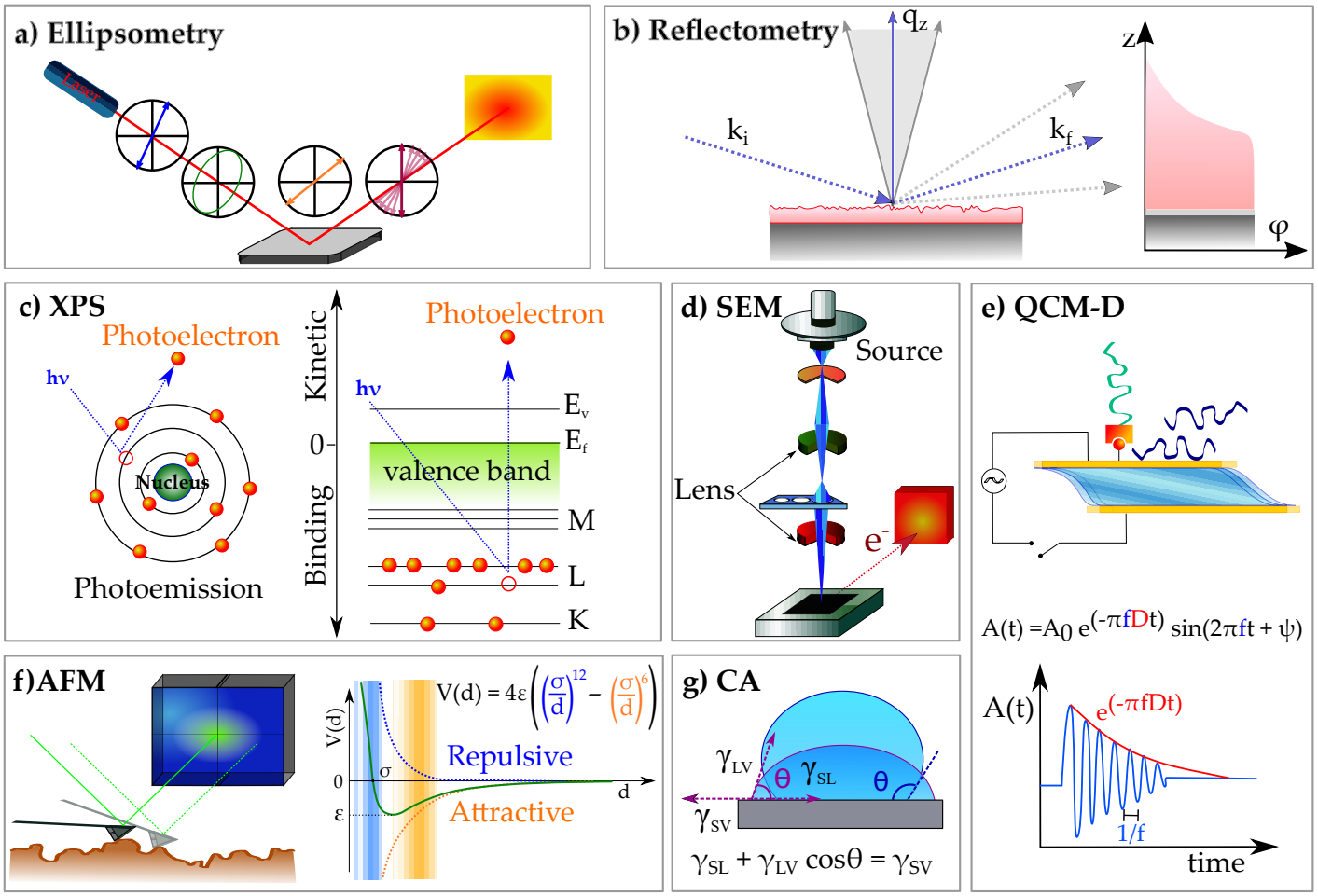

Fig. 7 Typical techniques for the characterization of thin films. (a) Ellipsometry is based on the detection of the change of polarization of light upon reflection from a substrate, which is described by the ellipsometric angles Δ and ψ. These parameters are related to the amplitude and the phase of the electromagnetic wave according to the fundamental equation $\tan\psi \cdot \exp^{i\Delta} = r_p/r_s$, with r_p and r_s the reflection coefficients of the perpendicular and parallel components of light. A layer model which describes the sample composition and its optical properties allow us to obtain the thickness d and refractive index n of the thin film from the experimental measurements. (b) Neutron or X-ray reflectometry provides information on the volume fraction distribution of molecules at interfaces. By measuring the reflected intensity of a probe (photons or neutrons) interacting with a solid surface at outgoing angles equal to the incoming one, a reflectivity profile in the reciprocal space, q_z, can be reconstructed. Characteristic structural parameters of a film, like thickness (d), roughness σ and refractive index, can be obtained by fitting the data to a proper model. The scattering properties of the components with respect to the incoming probe are described by the scattering length density ρ, which is correlated to the optical properties of the system by $\delta = \frac{\lambda^2}{2\pi}\rho$, with λ the probe wavelength. (c) X-ray photoelectron spectroscopy provides information on the chemical composition of a specimen adsorbed onto a surface. It is based on the photoemission of electrons from an excited sample, whose kinetic energy distribution is measured to derive chemical composition and electronic state of the sample surface. By total energy transfer from the photons to the core-level electrons of atomic or molecular orbitals, these electrons are emitted from the sample surface and are separated according to their energy, and so quantified. (d) Scanning electron microscopy uses a beam of electrons generated by an electron gun, and guided through within vacuum in an electromagnetic field towards the specimen surface the study the morphological properties of a surface. When the beam strikes the specimen surface, its high energy electrons interact with the valence electrons of the atoms in the sample, and these are ejected (secondary electrons). These electrons are then translated in changes of brightness of the corresponding point onto the screen, leading to the contrast of light and dark areas. (e) Quartz-crystal microbalance with dissipation monitoring (QCM-D) is a highly sensitive balance, which is able to detect nanograms of mass coupled to a substrate by detecting changes of the oscillation frequency of a quartz crystal. QCM-D uses the inverse piezoelectric effect, meaning that a driving sinusoidal potential is applied to a quartz crystal to excite the crystal oscillation forward and backward to its resonance frequency and higher overtones. When the potential is cut off, the damped amplitude of the freely decaying oscillation is recorded, and the frequency shift, Δf, and the dissipation energy, D, quantify coupled mass and energy dissipated by the specimen. (f) Atomic force microscopy (AFM) measures the interaction between a specimen and a solid probe scanning over the surface either in static or dynamic (oscillating) mode. From its deflection of the probe, morphological features from atomic to macroscopic (millimeters) scale can be explored. The mapping of the surface topology is a reconstruction of the interaction forces, with near-field forces approximated to Lennard-Jones potentials. (g) Contact angle measurements are performed by depositing a droplet of a liquid, in most cases water, onto a bare or modified surface to determine its wetting behavior, and therefore the surface hydrophilicity. The contact angle is defined as the geometrical angle between the substrate and the droplet, and it is correlated to the surface tension of all involved interfaces by the Young equation.

surface[176,177], with characteristic dry thickness from 5 to 50 nm from fully charged (CHI-Q_{100}) to partial (CHI-Q_{50}, CHI-Q_{25}) to neutral brushes, respectively, due to a decreased grafting density for higher charge density. An interesting property of polymer brushes is their swelling behavior, which can be exploited to design (bio) sensors and microactuators. These chitosan-based brushes have shown a variable swelling behavior over a broad pH range as a function of their quaternization form, with CHI-Q_{100} swelling up to 5 times their dry thickness at pH 5, and with an intermediate swelling degree symmetrically around this pH. Partially modified CHI-Q_{50} brushes were swelling symmetrically around pH 4.5, which is likely due to the balance between increasing protonation of primary amines below pH 6.5 and quaternary ammonium salts above pH 6.5. In contrast, the swelling of native chitosan and CH-Q_{25} was constant from pH 8.2 to 5.5, and increases near pH 4. The swelling behavior could be rationalised in terms of size of the counterions condensed around the charged groups: for fully protonated brushes, the swelling clearly increase with the size of counterions, while for partially protonated brushes the influence of the ions is evident at high pH, where there is a complete exchange of counterions from chloride to hydroxide, which have larger hydration shells. Such an effect is not visible for conditions of low pH and low degree of quaternization, where the ammonium cation content is below a critical value.

Chitosan brushes also exhibited a reduced bacterial attachment/growth of about 30 times compared to silane (APTES)-modified surface, which has been explained by the capability of the quaternary salt of disrupting the bacterial cell membrane, as well as by the flexible nature of polymer brush[178]. In fact, *S. aureus* biofilm adhered strongly to silicon oxide and CH surfaces even at high shear stress (up to 12 dyne per cm^2), whereas they detached at low shear stress (1.5 dyne per cm^2).

Brushes were prepared also from chitosan-grafted-poly(ethylenglycol) (PEG) copolymers[179,180], reaching very high degree of substitution, and adsorbed onto a thiol-modified gold substrate by microcontact printing, covalent grafting and solution adsorption, with the latter leading to the highest polymer adsorption. The presence of PEG units has been crucial to reach high surface adsorption, as revealed by QCM-D studies, and it enhances the hydration degree of chitosan thin films.

Chitosan-based nanocomposites and solid films

The combination of polymers and inorganic nanoparticles represents a well-known strategy to obtain hybrid materials with unique performances as well as specific functionalities. Among sustainable polymers, chitosan was largely employed as a matrix for the fabrication of bionanocomposites suitable for several applications, such as tissue engineering[181,182], drug delivery[183,184], gas sensors[185], packaging[186,187], remediation[188,189] and cultural heritage[190,191]. Such a wide industrial interest is related to some interesting features of chitosan itself in solid state. In particular, chitosan and its phosphorylated derivative are flame retardant and therefore they are perspective additives to control the flammability properties of polyethylene or to produce self-extinguishing cotton fabrics[192–194]. Additionally, chitosan, being

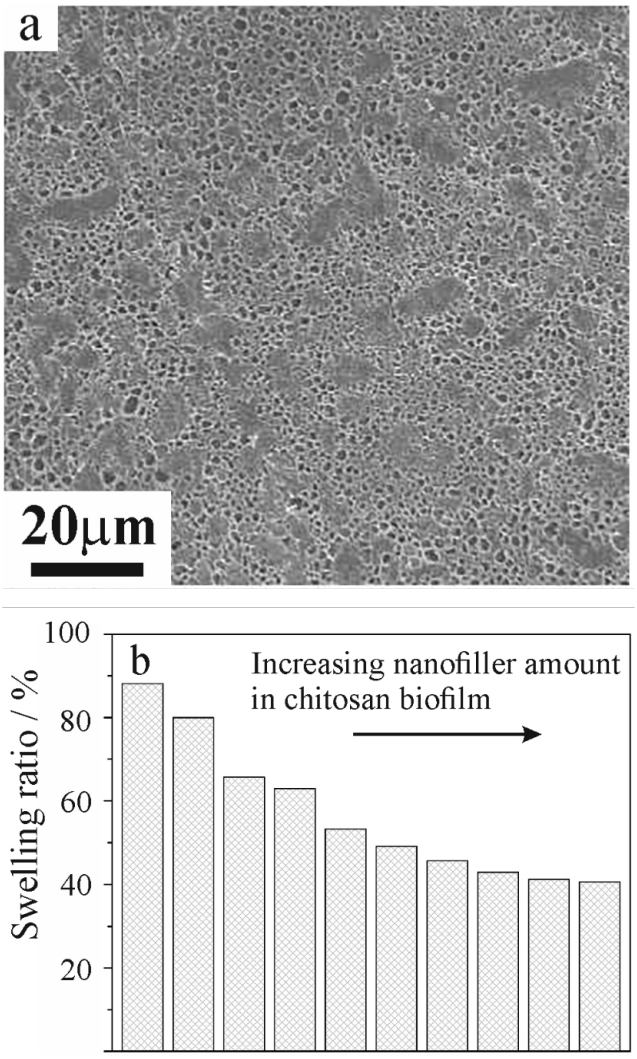

Fig. 8 (a) SEM image of the chitosan/HNTs-NH2 nanocomposite film containing ethylene glycol diglycidyl ether (EGDE) as cross-linking agent. (b) The swelling ratio of chitosan/HNTs-NH2 nanocomposite films. Adapted with permission from Ref. 181.

a polycation, has a broad-spectrum antimicrobial activity against both gram-positive, and gram-negative bacteria as well as fungi that can be further enhanced by transforming the primary amine groups into quaternary salts with permanent positive charge[195].

Mechanical performance of chitosan composites is affected by the crystallinity that has a great influence on tensile strength. Therefore, chitosan films fabricated through solvent casting from acetic acid may have significant differences in the mechanical properties if DDA, pH and water content in the final composite (Relative Humidity), which highly influence the polymer crystallinity, are altered[196,197].

Besides chemical modification of the chitosan structure, both natural and synthetic nanoparticles were successfully filled within the chitosan matrix to tune its properties. The nanocomposite preparation includes physical and chemical methods[199]. Metal nanoparticles (Cu, Ag and Au) were embedded in chitosan through the following subsequent steps[200]: 1) metal vapour synthesis for the preparation of the metal nanoparticles sols; 2) de-

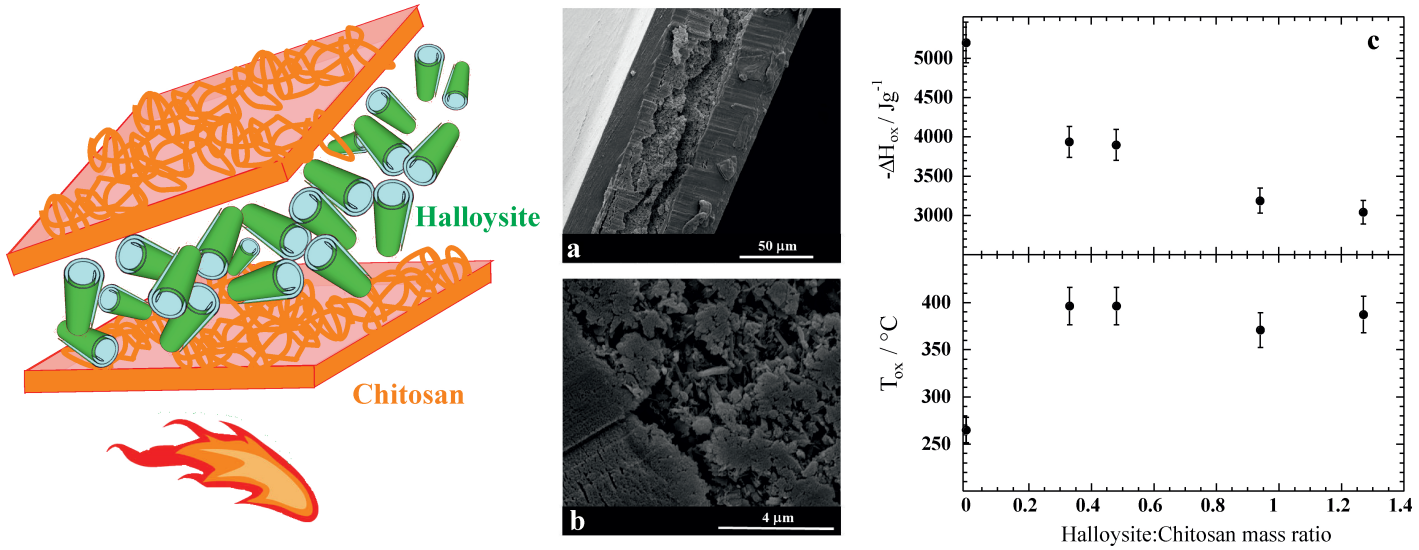

Fig. 9 Schematic representation of the chitosan/HNTs nanocomposites with a layered structure. (a, b) SEM micrographs at different magnification of the cross section of chitosan/HNT nanocomposites with a mass ratio of 0.62. (c) Enthalpy and onset temperature of oxidative degradation as functions of HNT/chitosan mass ratio for the layered nanocomposites. Adapted with permission from Ref. 198

position of the metal nanoparticles sols on chitosan supports. Chitosan/ZnO nanocomposites were fabricated by the microwave heating technique[188], which reduced the reaction time for the ligand substitution occurring between the functional groups of the biopolymer and the zinc cations of ZnO nanoparticles. The addition of ZnO nanoparticles improved the removal capacity of chitosan towards methylene blue[188]. The freeze-drying process was employed for the filling of nano-hydroxyapatite particles within chitosan matrix[201], while the ultrasonic-assisted method was used for the fabrication of composite scaffolds based on chitosan hydrogel and multiwalled carbon nanotubes (MWCNT)[182]. The addition of nano-hydroxyapatite improved the compression behaviour of the chitosan scaffold in terms of elasticity and flexibility[201]. A multifunctional hybrid material composed by chitosan, graphene oxide (GO) and iron oxide (IO) was obtained by the hydrothermal method exploiting the 1-ethyl-3-(3-dimethylaminopropyl) carbodiimide (EDC) reaction chemistry[202]. The chitosan-GO-IO nanocomposite revealed efficient antimicrobial ability towards both Gram-positive (Staphylococcus aureus) and Gram-negative (Escherichia coli) bacteria[202]. Due to its super-paramagnetic properties, the chitosan-GO-IO hybrid can be easily separated from the bacteria and reutilized for a subsequent biocide application[202].

Aqueous casting method was largely employed in the fabrication of chitosan based nanocomposites containing natural clay nanoparticles, such as kaolinite nanosheets[203,204] and halloysite nanotubes (HNTs)[204–206]. Literature[181] reports that the amino-modification of halloysite outer surface can favour the chitosan/HNTs interfacial interactions allowing to obtain hybrid films with excellent tensile and thermal properties. Additionally, the amino-modified clay nanotubes strongly improved the water vapour transmission rate of chitosan making the bionanocomposite films promising for biomedical purposes[181]. Ethylene glycol diglycidyl ether (EGDE) was used as cross-linker for the preparation of chitosan/amino-modified halloysite composite films. In the process, the hollow tubular shape of halloysite HNTs-NH_2 was not altered by the amino functionalization, and the composite film exhibits a porous structure, as shown by scanning electron microscopy (Fig. 8a). It was observed that the swelling ratio of chitosan based nanocomposites decreases with the HNTs-NH_2 content (Figure 8b).

Within tissue engineering applications, chitosan/halloysite composite scaffold was fabricated by the combination of solution-mixing and freeze-drying techniques[207]. The presence of clay nanotubes induced an improvement of both the compressive behaviour (in terms of strength and Young modulus) and the thermal stability with respect to the scaffold based on pristine chitosan[207]. Nanoclays with variable morphology (bentonite, sepiolite, and montmorillonite) were successfully filled into chitosan blended with glycerol by using the casting technique from water[208]. Similarly, chitosan/polyvinyl alcohol (PVA) blend was reinforced with different concentrations of bentonite nanoparticles combined with anthocyanin in order to obtain antibacterial films with improved thermo-mechanical performances[184]. The casting procedure was effective in the preparation of films composed by copper oxide (CuO) nanoparticles and chitosan doped with glycerol ionic liquid[185].

Recently, chitosan/halloysite nanocomposite films with a sandwich like structure, sketched in Figure 9a, were fabricated by using a sequential casting method[198]. The preparation protocol is based on the sequential deposition of chitosan and halloysite aqueous suspensions at controlled pH conditions. SEM images (Figure 9b) showed that the nanocomposite possesses a multilayer morphology being that halloysite nanotubes are confined between the outer chitosan layers. Compared to pure chitosan, a significant increase (up to ca. 150 °C) of the ignition temperature, as well as the enthalpy for the oxidation (Figure 9c) was detected in the hybrid films as a consequence of their layered structure[198].

The flame retardant features of materials where polymer and inorganic particles, typically clays, are alternated is well known but a large number of multilayers with micro/nanosized thickness is required[209], on the other hand the flame retardant features of the chitosan itself combined with the peculiar pH dependent solubility endow the reduction of flammability in more simple layered structures that are easy to generate. Accordingly, the sequential casting procedure can be considered a successful protocol to fabricate chitosan based nanocomposites with flame retardant properties.

Nanocomposite films formed by chitosan/polyvinyl alcohol (PVA) blend as matrix and graphene oxide/hydroxyapatite/gold nanoparticles as fillers were prepared by the gel casting method using glutaraldehyde as crossilinker[210]. These bionanocomposite films are promising for bone tissue regeneration as evidenced by the MTT essays and ALP straining results, which evidenced their capacity to enhance the osteoblast differentiation[210]. Within biomedical applications, the addition of rectorite clay particles into chitosan allowed to obtain a composite viscous mucus with injectable properties for skin hemostasis[211], whereas montmorillonite clay was introduced to methacrylated glycol chitosan (MeGC) hydrogel, which was obtained by using riboflavin as a photoinitiator[212]. The composite hydrogel evidenced a well interconnected microporous structure promoting the cell infiltration, proliferation, and in situ differentiation[212]. Hybrid gel beads based on chitosan and halloysite were prepared through the dropping and pH-precipitation method, which is based on the drop-wise addition of chitosan/halloysite dispersion into an aqueous NaOH solution[183,189]. The chitosan/HNTs gel beads exhibited higher adsorption capacities towards dyes (methylene blue and malachite green) with respect to those of chitosan gel beads[189]. As concerns pharmaceutical purposes, chitosan/HNTs gel beads revealed efficient in the controlled release of doxycycline (an antibiotic of the tetracycline class) highlighting their suitability as drug delivery system[189]. Interestingly, the drug release can be extended by covering the surface of the chitosan/HNTs gel beads with alginate exploiting the electrostatic attractions occurring between the biopolymers, which are oppositely charged[189]. Regarding Cultural Heritage, hybrid gels with surface cleaning ability were fabricated by mixing a chitosan aqueous solution with a Pickering emulsion based on HNTs and n-decane[190]. It should be noted that a subsequent drop-wise addition of NaOH solution was conducted to obtain the gel phase from the chitosan/HNTs/n-decane mixture[190].

Summary and perspectives

Chitosan exhibits a unique set of physico-chemical characteristics, most notably his low solubility, high intrinsic rigidity, large charge separation, strong tendency of forming intra- and intermolecular hydrogen bonds. In this contribution, an overview of recent advances in the chitosan-based materials are presented, whereby attention has been put to clarify how the peculiarities of chitosan affect the physico-chemical properties of the resulting materials.

The focus of the review was put on chitosan-based aqueous systems, thin films, and composite materials. Few polymers have attracted comparable attention and have been used for the design of so different systems. Accordingly, on overwhelming amount of literature appears each year on the topic. Similarly, the number of patents involving chitosan is continuously growing, indicating that chitosan does not only attract the interest of the scientific community but finds wide practical application. Chitosan is abundant (second to cellulose among biopolymers), competitive for physico-chemical properties and its use fits the idea of circular economy as it is a byproduct of food industry.

A contrast, commonly found in the field of material science, is that the rapid development of applications goes with a comparably slow progress in the understanding of the fundamental properties of the investigated system. Chitosan makes no exception to this rule. In fact, very fundamental questions about chitosan remain unanswered. For instance, a random distribution of N-acetylammine units along the polymer backbone is assumed, despite no evidence for chitosan being a random copolymer was ever presented. From the biological view point, the mechanisms of interaction of chitosan with cell, bacteria, and plants are not well understood and therefore a discrepancy in the reproducibility of bioactivity is observed. It seems clear that although several mechanism of action are reported, the most established idea is that electrostatic interactions between chitosan and anionic molecules of cell/DNA may control the bioactivity instead of interactions with a specific receptor.

Moreover, the interactions determining the behavior of hybrid systems can strongly vary: from non-specific, long range electrostatic, to more specific hydrogen bonds, to short-range and highly directional ionic bridges. Such a diversity makes systematic studies difficult to perform and predictions hardly apply to a broad variety of systems. Clearly, a better understanding of the behavior of this macromolecule is needed to improve our capacity to design chitosan-based materials. In conclusion, it generally true that the physical and chemical properties of the chitosan-based materials can be rationalized on the basis of the physico-chemical properties of this important bio-macromolecule. It is equally true, that further fundamental and applied studies are required to improve our capacity to predict the properties of highly complex, multi-component, chitosan based materials.

Conflicts of interest

There are no conflicts to declare.

Acknowledgements

The work was financially supported by Progetto di ricerca e sviluppo "AGM for CuHe" (ARS01_00697) and University of Palermo. Experimental work performed on chitosan-fatty acid complexes and thin films have profited from the laboratory infrastructure provided by the Partnership of Soft Condensed Matter (PSCM) at the Institut Laue-Langevin.

Notes and references

1 M. Rinaudo, *Progress in Polymer Science*, 2006, **31**, 603–632.
2 C. Tang, N. Chen, Q. Zhang, K. Wang, Q. Fu and X. Zhang, *Polymer Degradation and Stability*, 2009, **94**, 124–131.
3 K. B. Mukhtar Ahmed, M. M. A. Khan, H. Siddiqui and A. Jahan, *Carbohydrate Polymers*, 2020, **227**, 115331.

4 M. Rinaudo, M. Milas and P. Le Dung, *International Journal of Biological Macromolecules*, 1993, **15**, 281–285.

5 C. Schatz, C. Viton, T. Delair, C. Pichot and A. Domard, *Biomacromolecules*, 2003, **4**, 641–648.

6 H. Wang, J. Qian and F. Ding, *Journal of Materials Chemistry B*, 2017, **5**, 6986–7007.

7 Y. P. Singh, J. C. Moses, N. Bhardwaj and B. B. Mandal, *Journal of Materials Chemistry B*, 2018, **6**, 5499–5529.

8 F. Khan, D. T. N. Pham, S. F. Oloketuyi, P. Manivasagan, J. Oh and Y.-M. Kim, *Colloids and Surfaces B: Biointerfaces*, 2020, **185**, 110627.

9 W. Zhang, H. Wang, X. Hu, H. Feng, W. Xiong, W. Guo, J. Zhou, A. Mosa and Y. Peng, *Journal of Cleaner Production*, 2019, **231**, 733–745.

10 L. Xing, Y.-T. Fan, L.-J. Shen, C.-X. Yang, X.-Y. Liu, Y.-N. Ma, L.-Y. Qi, K.-H. Cho, C.-S. Cho and H.-L. Jiang, *International Journal of Biological Macromolecules*, 2019, **141**, 85–97.

11 M. Nasrollahzadeh, N. Shafiei, Z. Nezafat, N. S. Soheili Bidgoli and F. Soleimani, *Carbohydrate Polymers*, 2020, **241**, 116353.

12 L. Xu, C. Wang, Y. Cui, A. Li, Y. Qiao and D. Qiu, *Science Advances*, 2019, **5**, eaau3442.

13 M. Rinaudo, N. R. Kil'deeva and V. G. Babak, *Russian Journal of General Chemistry*, 2008, **78**, 2239–2246.

14 L. Chiappisi, I. Hoffmann and M. Gradzielski, *Soft Matter*, 2013, **9**, 3896–3909.

15 L. Chiappisi and M. Gradzielski, *Advances in Colloid and Interface Science*, 2015, **220**, 92–107.

16 C. Onesippe and S. Lagerge, *Carbohydrate Polymers*, 2008, **74**, 648–658.

17 Y. C. Wei and S. M. Hudson, *Macromolecules*, 1993, **26**, 4151–4154.

18 L. Petrović, J. Milinković, J. Fraj, S. Bučko, J. Katona and L. Spasojević, *Colloid Polym. Sci.*, 2017, **295**, 2279–2285.

19 S. Peretz, M. Florea-Spiroiu, D.-F. Anghel, C. Munteanu, D. Angelescu, C. Stoian and G. Zgherea, *Journal of Applied Polymer Science*, 2014, **131**, 40059.

20 P. Pal and A. Pal, *International Journal of Biological Macromolecules*, 2017, **104**, 1548–1555.

21 S. Demarger-André and A. Domard, *Carbohydrate Polymers*, 1994, **23**, 211–219.

22 M. C. Bonferoni, G. Sandri, E. Dellera, S. Rossi, F. Ferrari, M. Mori and C. Caramella, *European Journal of Pharmaceutics and Biopharmaceutics*, 2014, **87**, 101–106.

23 M. Vargas, A. Albors, A. Chiralt and C. González-Martínez, *Food Hydrocolloids*, 2009, **23**, 536–547.

24 E. Dellera, M. C. Bonferoni, G. Sandri, S. Rossi, F. Ferrari, C. Del Fante, C. Perotti, P. Grisoli and C. Caramella, *European Journal of Pharmaceutics and Biopharmaceutics*, 2014, **88**, 643–650.

25 M. V. Shamov, S. Y. Y. Bratskaya and V. A. Avramenko, *Journal of colloid and interface science*, 2002, **249**, 316–321.

26 S. Demarger-André and A. Domard, *Carbohydrate Polymers*, 1995, **27**, 101–107.

27 I. Ahmed, L. Dildar, A. Haque, P. Patra, M. Mukhopadhyay, S. Hazra, M. Kulkarni, S. Thomas, J. R. Plaisier, S. B. Dutta and J. K. Bal, *Journal of Colloid and Interface Science*, 2018, **514**, 433–442.

28 M. Hasan, G. Ben Messaoud, F. Michaux, A. Tamayol, C. J. F. Kahn, N. Belhaj, M. Linder and E. Arab-Tehrany, *RSC Advances*, 2016, **6**, 45290–45304.

29 H. W. Tan and M. Misran, *Journal of liposome research*, 2012, **22**, 329–335.

30 L. Chiappisi, S. Prévost, I. Grillo and M. Gradzielski, *Langmuir*, 2014, **30**, 1778–1787.

31 L. Chiappisi, S. Prévost, I. Grillo and M. Gradzielski, *Langmuir*, 2014, **30**, 10608–10616.

32 L. Chiappisi, S. David Leach, M. Gradzielski, S. D. Leach and M. Gradzielski, *Soft Matter*, 2017, **13**, 4988–4996.

33 S. Micciulla, D. W. Hayward, Y. Gerelli, A. Panzarella, R. von Klitzing, M. Gradzielski and L. Chiappisi, *Communications Chemistry*, 2019, **2**, 61.

34 L. Chiappisi, M. Simon and M. Gradzielski, *ACS Applied Materials & Interfaces*, 2015, **7**, 6139–6145.

35 M. Valtiner, S. H. Donaldson, M. A. Gebbie and J. N. Israelachvili, *Journal of the American Chemical Society*, 2012, **134**, 1746–1753.

36 J. H. J. Hamman, *Marine drugs*, 2010, **8**, 1305–1322.

37 Y. Luo and Q. Wang, *International Journal of Biological Macromolecules*, 2014, **64**, 353–367.

38 P. Pakornpadungsit, T. Prasopdee, N. M. Swainson, A. Chworos and W. Smitthipong, *Polymer Testing*, 2020, **83**, 106333.

39 L. M. Bravo-Anaya, K. G. Fernández-Solís, J. Rosselgong, J. L. E. Nano-Rodríguez, F. Carvajal and M. Rinaudo, *International Journal of Biological Macromolecules*, 2019, **126**, 1037–1049.

40 P. L. Ma, M. Lavertu, F. M. Winnik and M. D. Buschmann, *Carbohydrate Polymers*, 2017, **176**, 167–176.

41 J.-W. Shen, J. Li, Z. Zhao, L. Zhang, G. Peng and L. Liang, *Scientific Reports*, 2017, **7**, 5050.

42 P. L. Ma, M. Lavertu, F. M. Winnik, M. D. Buschmann, L. M. Pei, M. Lavertu, F. M. Winnik and M. D. Buschmann, *Biomacromolecules*, 2009, **10**, 1490–1499.

43 H. Ragelle, R. Riva, G. Vandermeulen, B. Naeye, V. Pourcelle, C. S. Le Duff, C. D'Haese, B. Nysten, K. Braeckmans, S. De Smedt, C. Jérôme and V. Préat, *Journal of Controlled Release*, 2014, **176**, 54–63.

44 I. Pilipenko, V. Korzhikov-Vlakh, V. Sharoyko, N. Zhang, M. Schäfer-Korting, E. Rühl, C. Zoschke and T. Tennikova, *Pharmaceutics*, 2019, **11**, 317.

45 C. Zandanel, M. Noiray and C. Vauthier, *Pharmaceutical Research*, 2020, **37**, 22.

46 P. Holzerny, B. Ajdini, W. Heusermann, K. Bruno, M. Schuleit, L. Meinel and M. Keller, *Journal of Controlled Release*, 2012, **157**, 297–304.

47 S. Reed and B. M. Wu, *Journal of Biomedical Materials Research Part B: Applied Biomaterials*, 2017, **105**, 272–282.

48 K. Xu, K. Ganapathy, T. Andl, Z. Wang, J. A. Copland, R. Chakrabarti and S. J. Florczyk, *Biomaterials*, 2019, **217**, 119311.

49 E. A. Krisanti, G. M. Naziha, N. S. Amany, K. Mulia and N. A. Handayani, *IOP Conference Series: Materials Science and Engineering*, 2019, **509**, 012100.

50 M. Kuczajowska-Zadrożna, U. Filipkowska and T. Jóźwiak, *Journal of Environmental Chemical Engineering*, 2020, 103878.

51 A. B. Kayitmazer, A. F. Koksal and E. Kilic Iyilik, *Soft matter*, 2015, **11**, 8605–12.

52 O. Karabiyik Acar, A. B. Kayitmazer and G. Torun Kose, *Biomacromolecules*, 2018, **19**, 1198–1211.

53 C. Schatz, J.-M. Lucas, C. Viton, A. Domard, C. Pichot and T. Delair, *Langmuir*, 2004, **20**, 7766–7778.

54 J. Valente, V. Gaspar, B. Antunes, P. Countinho and I. Correia, *Polymer*, 2013, **54**, 5–15.

55 P. M. de la Torre, S. Torrado and S. Torrado, *Biomaterials*, 2003, **24**, 1459–1468.

56 Q. Chen, Y. Hu, Y. Chen, X. Jiang and Y. Yang, *Macromolecular Bioscience*, 2005, **5**, 993–1000.

57 Y. Hu, X. Jiang, Y. Ding, H. Ge, Y. Yuan and C. Yang, *Biomaterials*, 2002, **23**, 3193–3201.

58 R.-Y. Zhang, E. Zaslavski, G. Vasilyev, M. Boas and E. Zussman, *Biomacromolecules*, 2018, **19**, 588–595.

59 D. Chuan, T. Jin, R. Fan, L. Zhou and G. Guo, *Advances in Colloid and Interface Science*, 2019, **268**, 25–38.

60 S. P. Strand, S. Lelu, N. K. Reitan, C. de Lange Davies, P. Artursson and K. M. Vårum, *Biomaterials*, 2010, **31**, 975–987.

61 C. Cui, C. Shao, L. Meng and J. Yang, *ACS Applied Materials & Interfaces*, 2019, **11**, 39228–39237.

62 S. Gokila, T. Gomathi, P. Sudha and S. Anil, *International Journal of Biological Macromolecules*, 2017, **104**, 1459–1468.

63 D. P. Facchi, A. L. Cazetta, E. A. Canesin, V. C. Almeida, E. G. Bonafé, M. J. Kipper and A. F. Martins, *Chemical Engineering Journal*, 2018, **337**, 595–608.

64 F.-L. Mi, H.-W. Sung and S.-S. Shyu, *Carbohydrate Polymers*, 2002, **48**, 61–72.

65 K. Baysal, A. Z. Aroguz, Z. Adiguzel and B. M. Baysal, *International Journal of Biological Macromolecules*, 2013, **59**, 342–348.

66 W. Zhang, X. Jin, H. Li, R.-r. Zhang and C.-w. Wu, *Carbohydrate Polymers*, 2018, **186**, 82–90.

67 A. Drogoz, L. David, C. Rochas, A. Domard and T. Delair, *Langmuir*, 2007, **23**, 10950–10958.

68 R. Rodríguez-Rodríguez, H. Espinosa-Andrews, C. Velasquillo-Martínez and Z. Y. García-Carvajal, *International Journal of Polymeric Materials and Polymeric Biomaterials*, 2020, **69**, 1–20.

69 H. Hamedi, S. Moradi, S. M. Hudson and A. E. Tonelli, *Carbohydrate Polymers*, 2018, **199**, 445–460.

70 P. Mohammadzadeh Pakdel and S. J. Peighambardoust, *Carbohydrate Polymers*, 2018, **201**, 264–279.

71 N. Sereni, A. Enache, G. Sudre, A. Montembault, C. Rochas, P. Durand, M. H. Perrard, G. Bozga, J. P. Puaux, T. Delair and L. David, *Langmuir*, 2017, **33**, 12697–12707.

72 A. A. Enache, L. David, J. P. Puaux, I. Banu and G. Bozga, *Journal of Applied Polymer Science*, 2018, **135**, 1–12.

73 P. Sacco, F. Brun, I. Donati, D. Porrelli, S. Paoletti and G. Turco, *ACS Applied Materials and Interfaces*, 2018, **10**, 10761–10770.

74 Y. Huang, Y. Cai and Y. Lapitsky, *Journal of Materials Chemistry B*, 2015, **3**, 5957–5970.

75 P. Sacco, S. Paoletti, M. Cok, F. Asaro, M. Abrami, M. Grassi and I. Donati, *International Journal of Biological Macromolecules*, 2016, **92**, 476–483.

76 L. Bugnicourt and C. Ladavière, *Progress in Polymer Science*, 2016, **60**, 1–17.

77 L. Dambies, T. Vincent, A. Domard and E. Guibal, *Biomacromolecules*, 2001, **2**, 1198–1205.

78 Azizullah, N. ur Rehman, A. Haider, U. Kortz, S. U. Afridi, M. Sohail, S. A. Joshi and J. Iqbal, *International Journal of Pharmaceutics*, 2017, **533**, 125–137.

79 X. Z. Shu and K. J. Zhu, *International Journal of Pharmaceutics*, 2002, **233**, 217–225.

80 S. Saravanan, S. Vimalraj, P. Thanikaivelan, S. Banudevi and G. Manivasagam, *International Journal of Biological Macromolecules*, 2019, **121**, 38–54.

81 H. Y. Zhou, L. J. Jiang, P. P. Cao, J. B. Li and X. G. Chen, *Carbohydrate Polymers*, 2015, **117**, 524–536.

82 Aihua Shi, X. Dai and Z. Jing, *Polymer Science, Series A*, 2020, **62**, 228–239.

83 G. A. F. Roberts and K. E. Taylor, *Makro*, 1989, **190**, 951–960.

84 P. Hu, C. B. Raub, J. S. Choy and X. Luo, *J. Mater. Chem. B*, 2020, **8**, 2519–2529.

85 L. Gao, H. Gan, Z. Meng, R. Gu, Z. Wu, L. Zhang, X. Zhu, W. Sun, J. Li, Y. Zheng and G. Dou, *Colloids and Surfaces B: Biointerfaces*, 2014, **117**, 398–405.

86 R. A. Muzzarelli, M. El Mehtedi, C. Bottegoni, A. Aquili and A. Gigante, *Marine Drugs*, 2015, **13**, 7314–7338.

87 G. Tripodo, A. Trapani, A. Rosato, C. Di Franco, R. Tamma, G. Trapani, D. Ribatti and D. Mandracchia, *Carbohydrate Polymers*, 2018, **198**, 124–130.

88 L. Pérez-Álvarez, L. Ruiz-Rubio, B. Artetxe, M. d.M. Vivanco, J. M. Gutiérrez-Zorrilla and J. L. Vilas-Vilela, *Carbohydrate Polymers*, 2019, **213**, 159–167.

89 L. Li, N. Wang, X. Jin, R. Deng, S. Nie, L. Sun, Q. Wu, Y. Wei and C. Gong, *Biomaterials*, 2014, **35**, 3903–3917.

90 E. A. Kamoun, *Journal of Advanced Research*, 2016, **7**, 69–77.

91 E. Lucas de Lima, N. Fittipaldi Vasconcelos, J. da Silva Maciel, F. Karine Andrade, R. Silveira Vieira and J. P. Andrade Feitosa, *Journal of Materials Science: Materials in Medicine*, 2020, **31**, 5.

92 J. Berger, M. Reist, J. M. Mayer, O. Felt, N. A. Peppas and R. Gurny, *European Journal of Pharmaceutics and Biopharmaceutics*, 2004, **57**, 19–34.

93 L. Weng, X. Chen and W. Chen, *Biomacromolecules*, 2007, **8**, 1109–1115.

94 P. Sautrot-Ba, N. Razza, L. Breloy, S. A. Andaloussi, A. Chiappone, M. Sangermano, C. Hélary, S. Belbekhouche, T. Coradin and D. L. Versace, *Journal of Materials Chemistry B*, 2019, **7**, 6526–6538.

95 M. Pei, J. Mao, W. Xu, Y. Zhou and P. Xiao, *Journal of Polymer Science Part A: Polymer Chemistry*, 2019, **57**, 1862–1871.

96 J. Huang, J. Qin, P. Zhang, X. Chen, X. You, F. Zhang, B. Zuo and M. Yao, *Carbohydrate Polymers*, 2020, **229**, 115515.

97 A. K. Ospanova, B. E. Savdenbekova, M. K. Iskakova, R. A. Omarova, R. N. Zhartybaev, B. Z. Nussip and A. S. Abdikadyr, *IOP Conf. Ser. Mater. Sci. Eng.*, 2017, **230**, 1–6.

98 M. T. Cook, G. Tzortzis, V. V. Khutoryanskiy and D. Charalampopoulos, *J. Mater. Chem. B*, 2013, **1**, 52–60.

99 K. Tian, C. Xie and X. Xia, *Colloids Surfaces B Biointerfaces*, 2013, **109**, 82–89.

100 J. H. Bongaerts, J. J. Cooper-White and J. R. Stokes, *Biomacromolecules*, 2009, **10**, 1287–1294.

101 M. Criado-Gonzalez, M. Fernandez-Gutierrez, J. San Roman, C. Mijangos and R. Hernández, *Carbohydrate Polymers*, 2019, **206**, 428–434.

102 A. Ali and S. Ahmed, *Int. J. Biol. Macromol.*, 2018, **109**, 273–286.

103 L. Pérez-Álvarez, L. Ruiz-Rubio, I. Azua, V. Benito, A. Bilbao and J. L. Vilas-Vilela, *Eur. Polym. J.*, 2019, **112**, 31–37.

104 B. Guan, H. Wang, R. Xu, G. Zheng, J. Yang, Z. Liu, M. Cao, M. Wu, J. Song, N. Li, T. Li, Q. Cai, X. Yang, Y. Li and X. Zhang, *Sci. Rep.*, 2016, **6**, 1–12.

105 H. Lv, Z. Chen, X. Yang, L. Cen, X. Zhang and P. Gao, *J. Dent.*, 2014, **42**, 1464–1472.

106 S. Del Hoyo-Gallego, L. Pérez-Álvarez, F. Gómez-Galván, E. Lizundia, I. Kuritka, V. Sedlarik, J. M. Laza and J. L. Vila-Vilela, *Carbohydr. Polym.*, 2016, **143**, 35–43.

107 V. Nascimento, C. França, J. Hernández-Montelongo, D. Machado, M. Lancellotti, M. Cotta, R. Landers and M. Beppu, *Eur. Polym. J.*, 2018, **109**, 198–205.

108 L. Maddalena, F. Carosio, J. Gomez, G. Saracco and A. Fina, *Polym. Degrad. Stab.*, 2018, **152**, 1–9.

109 J. Jung, L. Li, C. K. Yeh, X. Ren and Y. Sun, *Mater. Sci. Eng. C*, 2019, **104**, 109961.

110 H. Wang, J. Qian and F. Ding, *J. Agric. Food Chem.*, 2018, **66**, 395–413.

111 S. Kumar, A. Mukherjee and J. Dutta, *Trends Food Sci. Technol.*, 2020, **97**, 196–209.

112 N. L. Benbow, J. L. Webber, S. Karpiniec, M. Krasowska, J. K. Ferri and D. A. Beattie, *Phys. Chem. Chem. Phys.*, 2017, **19**, 23790–23801.

113 T. I. Croll, A. J. O'Connor, G. W. Stevens and J. J. Cooper-White, *Biomacromolecules*, 2006, **7**, 1610–1622.

114 J. J. Richardson, M. Bjornmalm and F. Caruso, *Science*, 2015, **348**, aaa2491–9.

115 H. Kaygusuz, S. Micciulla, F. B. Erim and R. von Klitzing, *J. Polym. Sci. Part B Polym. Phys.*, 2017, **55**, 1798–1803.

116 J. Huang, S. Zajforoushan Moghaddam and E. Thormann, *ACS Omega*, 2019, **4**, 2019–2029.

117 G. Decher, *Science*, 1997, **277**, 1232–1237.

118 J. B. Schlenoff, A. H. Rmaile and C. B. Bucur, *J. Am. Chem. Soc.*, 2008, **130**, 13589–13597.

119 R. v. Klitzing, *Phys. Chem. Chem. Phys.*, 2006, **8**, 5012.

120 D. Volodkin and R. von Klitzing, *Curr. Opin. Colloid Interface Sci.*, 2014, 1–7.

121 C. Coquery, F. Carosio, C. Negrell, N. Caussé, N. Pébère and G. David, *Surfaces and Interfaces*, 2019, **16**, 59–66.

122 W. Yuan, H. Dong, C. M. Li, X. Cui, L. Yu, Z. Lu and Q. Zhou, *Langmuir*, 2007, **23**, 13046–13052.

123 J. M. Silva, A. R. C. Duarte, S. G. Caridade, C. Picart, R. L. Reis and J. F. Mano, *Biomacromolecules*, 2014, **15**, 3817–26.

124 G. Maurstad, Y. A. Mørch, A. R. Bausch and B. T. Stokke, *Carbohydr. Polym.*, 2008, **71**, 672–681.

125 P. Kujawa, P. Moraille, J. Sanchez, A. Badia and F. M. Winnik, *J. Am. Chem. Soc.*, 2005, **127**, 9224–9234.

126 T. Tariverdian, T. Navaei, P. B. Milan, A. Samadikuchaksaraei and M. Mozafari, *Advanced Functional Polymers for Biomedical Applications*, Elsevier, 2019, pp. 323–357.

127 J. A. Burdick and G. D. Prestwich, *Adv. Mater.*, 2011, **23**, 41–56.

128 H. H. Trimm and B. R. Jennings, *Biochem. J.*, 1983, **213**, 671–677.

129 N. Ghavidel Mehr, C. D. Hoemann and B. D. Favis, *Polymer*, 2015, **64**, 112–121.

130 J. Choi and M. F. Rubner, *Macromolecules*, 2005, **38**, 116–124.

131 M. Elzbieciak, S. Zapotoczny, P. Nowak, R. Krastev, M. Nowakowska and P. Warszyński, *Langmuir*, 2009, **25**, 3255–3259.

132 E. Guzmán, J. A. Cavallo, R. Chuliá-Jordán, C. Gómez, M. C. Strumia, F. Ortega and R. G. Rubio, *Langmuir*, 2011, **27**, 6836–6845.

133 C. Huang, G. Fang, Y. Zhao, S. Bhagia, X. Meng, Q. Yong and A. J. Ragauskas, *Carbohydr. Polym.*, 2019, **222**, 115036.

134 U. Voigt, V. Khrenov, K. Tauer, M. Hahn, W. Jaeger and R. V. Klitzing, *J. Phys. Condens. Matter*, 2003, **15**, S213—-S218.

135 S. Micciulla, S. Dodoo, C. Chevigny, A. Laschewsky and R. von Klitzing, *Phys. Chem. Chem. Phys.*, 2014, **16**, 21988–21998.

136 L. Richert, P. Lavalle, E. Payan, X. Z. Shu, G. D. Prestwich, J. F. Stoltz, P. Schaaf, J. C. Voegel and C. Picart, *Langmuir*, 2004, **20**, 448–458.

137 C. Picart, J. Mutterer, L. Richert, Y. Luo, G. D. Prestwich, P. Schaaf, J.-C. C. Voegel and P. Lavalle, *Proceedings of the National Academy of Sciences of the United States of America*, 2002, **99**, 12531–12535.

138 M. Zerball, A. Laschewsky and R. Von Klitzing, *Journal of Physical Chemistry B*, 2015, **119**, 11879–11886.

139 C. Liu, E. Thormann, P. M. Claesson and E. Tyrode, *Langmuir*, 2014, **30**, 8866–8877.

140 K. Wulf, S. Schünemann, A. Strohbach, R. Busch, S. B. Felix,

K. P. Schmitz, K. Sternberg and S. Petersen, *BioNanoMaterials*, 2015, **16**, 265–273.
141 J. M. Silva, S. G. Caridade, N. M. Oliveira, R. L. Reis and J. F. Mano, *J. Mater. Chem. B*, 2015, **3**, 4555–4568.
142 N. M. Alves, C. Picart and J. F. Mano, *Macromol. Biosci.*, 2009, **9**, 776–785.
143 G. V. Martins, E. G. Merino, J. F. Mano and N. M. Alves, *Macromol. Biosci.*, 2010, **10**, 1444–1455.
144 A. F. Martins, J. Vlcek, T. Wigmosta, M. Hedayati, M. M. Reynolds, K. C. Popat and M. J. Kipper, *Appl. Surf. Sci.*, 2020, **502**, 144282.
145 M. Marudova, S. Lang, G. J. Brownsey and S. G. Ring, *Carbohydr. Res.*, 2005, **340**, 2144–2149.
146 A. E. Sorkio, E. P. Vuorimaa-Laukkanen, H. M. Hakola, H. Liang, T. A. Ujula, J. J. Valle-Delgado, M. Österberg, M. L. Yliperttula and H. Skottman, *Biomaterials*, 2015, **51**, 257–269.
147 M. Andonegi, K. L. Heras, E. Santos-Vizcaíno, M. Igartua, R. M. Hernandez, K. de la Caba and P. Guerrero, *Carbohydr. Polym.*, 2020, **237**, 116159.
148 I. Leceta, P. Arana, P. Guerrero and K. De La Caba, *Materials Letters*, 2014, **128**, 125–127.
149 A. Sionkowska and A. Płanecka, *J. Mol. Liq.*, 2013, **186**, 157–162.
150 T. Yovcheva, B. Pilicheva, A. Marinova, A. Viraneva, I. Bodurov, G. Exner, S. Sotirov, I. Vlaeva, Y. Uzunova and M. Marudova, *J. Phys. Conf. Ser.*, 2019, **1186**, 1–7.
151 K. Junka, O. Sundman, J. Salmi, M. Österberg and J. Laine, *Carbohydr. Polym.*, 2014, **108**, 34–40.
152 K. Cai, Y. Hu, Y. Wang and L. Yang, *J Biomed Mater Res*, 2008, **84A**, 516–522.
153 A. Dedinaite, M. Lundin, L. Macakova and T. Auletta, *Langmuir*, 2005, **21**, 9502–9509.
154 H. Huang and X. Yang, *Colloids and Surfaces A: Physicochemical and Engineering Aspects*, 2003, **226**, 77–86.
155 A. Valverde, L. Pérez-Álvarez, L. Ruiz-Rubio, M. A. Pacha Olivenza, M. B. García Blanco, M. Díaz-Fuentes and J. L. Vilas-Vilela, *Carbohydr. Polym.*, 2019, **207**, 824–833.
156 H. Zare, G. D. Najafpour, M. Jahanshahi, M. Rahimnejad and M. Rezvani, *Rom. Biotechnol. Lett.*, 2017, **22**, 12611–12619.
157 H. Sun, D. Choi, J. Heo, S. Y. Jung and J. Hong, *Cancers (Basel).*, 2020, **12**, 1–14.
158 P. Li, Y.-N. Dai, J.-P. Zhang, A.-Q. Wang and Q. Wei, *International journal of biomedical science : IJBS*, 2008, **4**, 221–8.
159 I. M. Brasil, C. Gomes, A. Puerta-Gomez, M. E. Castell-Perez and R. G. Moreira, *LWT - Food Sci. Technol.*, 2012, **47**, 39–45.
160 Y. Kusumastuti, A. Istiani, Rochmadi and C. W. Purnomo, *Adv. Mater. Sci. Eng.*, 2019, **2019**, 1–8.
161 J. B. Schlenoff, S. T. Dubas and T. Farhat, *Langmuir*, 2000, **16**, 9968–9969.
162 K. C. Krogman, N. S. Zacharia, S. Schroeder and P. T. Hammond, *Langmuir*, 2007, **23**, 3137–3141.
163 K. C. Krogman, J. l. Lowery, N. S. Zacharia, G. C. Rutledge and P. T. Hammond, *Nat. Mater.*, 2009, **8**, 512–518.
164 A. Izquierdo, S. S. Ono, J.-C. C. Voegel, P. Schaaf and G. Decher, *Langmuir*, 2005, **21**, 7558–67.
165 M. Kolasinska, R. Krastev, T. Gutberlet and P. Warszynski, *Langmuir*, 2009, **25**, 1224–1232.
166 M. Criado, E. Rebollar, A. Nogales, T. A. Ezquerra, F. Boulmedais, C. Mijangos and R. Hernández, *Biomacromolecules*, 2017, **18**, 169–177.
167 M. Bulwan, S. Zapotoczny and M. Nowakowska, *Soft Matter*, 2009, **5**, 4726–4732.
168 I. Langmuir, *J. Am. Chem. Soc.*, 1917, **39**, 1848–1906.
169 K. B. Blodgett, *J. Am. Chem. Soc.*, 1935, **57**, 1007–1022.
170 F. J. Pavinatto, L. Caseli and O. N. Oliveira, *Biomacromolecules*, 2010, **11**, 1897–908.
171 P. T. Hammond, *Advanced Materials*, 2004, **16**, 1271–1293.
172 Y. Sakai-Otsuka, S. Zaioncz, I. Otsuka, S. Halila, P. Rannou and R. Borsali, *Macromolecules*, 2017, **50**, 3365–3376.
173 Y. Liao, W.-C. Chen and R. Borsali, *Advanced Materials*, 2017, **29**, 1701645.
174 N. Ayres, *Polym. Chem.*, 2010, **1**, 769–777.
175 O. Azzaroni, *J. Polym. Sci. Part A Polym. Chem.*, 2012, **50**, 3225–3258.
176 H. S. Lee, D. M. Eckmann, D. Lee, N. J. Hickok and R. J. Composto, *Langmuir*, 2011, **27**, 12458–12465.
177 H. S. Lee, M. Q. Yee, Y. Y. Eckmann, N. J. Hickok, D. M. Eckmann and R. J. Composto, *J. Mater. Chem.*, 2012, **22**, 19605–19616.
178 P. Kurt, L. Wood, D. E. Ohman and K. J. Wynne, *Langmuir*, 2007, **23**, 4719–4723.
179 N. Gorochovceva, A. Naderi, A. Dedinaite and R. Makuška, *Eur. Polym. J.*, 2005, **41**, 2653–2662.
180 Y. Zhou, B. Liedberg, N. Gorochovceva, R. Makuska, A. Dedinaite and P. M. Claesson, *J. Colloid Interface Sci.*, 2007, **305**, 62–71.
181 M. Xie, K. Huang, F. Yang, R. Wang, L. Han, H. Yu, Z. Ye and F. Wu, *International Journal of Biological Macromolecules*, 2020, **151**, 1116–1125.
182 S. Velmurugan, S. Palanisamy, T. C-K Yang, M. Gochoo and S.-W. W. Chen, *Ultrasonics Sonochemistry*, 2020, **62**, 104863.
183 L. Lisuzzo, G. Cavallaro, F. Parisi, S. Milioto, R. Fakhrullin and G. Lazzara, *Coatings*, 2019, **9**, 70.
184 M. Koosha and S. Hamedi, *Progress in Organic Coatings*, 2019, **127**, 338–347.
185 F. I. Ali, S. T. Mahmoud, F. Awwad, Y. E. Greish and A. F. Abu-Hani, *Carbohydrate Polymers*, 2020, **236**, 116064.
186 A. Giannakas, P. Stathopoulou, G. Tsiamis and C. Salmas, *Journal of Food Processing and Preservation*, 2020, **44**, year.
187 V. Labonté, A. Marion, N. Virgilio and J. R. Tavares, *Industrial & Engineering Chemistry Research*, 2016, **55**, 7362–7372.
188 M. H. Mostafa, M. A. Elsawy, M. S. Darwish, L. I. Hussein and A. H. Abdaleem, *Materials Chemistry and Physics*, 2020, **248**, 122914.
189 Q. Peng, M. Liu, J. Zheng and C. Zhou, *Microporous and*

Mesoporous Materials, 2015, **201**, 190–201.

190 G. Cavallaro, S. Milioto, L. Nigamatzyanova, F. Akhatova, R. Fakhrullin and G. Lazzara, *ACS Applied Nano Materials*, 2019, **2**, 3169–3176.

191 G. Cavallaro, S. Milioto and G. Lazzara, *Langmuir*, 2020, **36**, 3677–3689.

192 G. Cavallaro, G. Lazzara, S. Konnova, R. Fakhrullin and Y. Lvov, *Green Materials*, 2014, **2**, 232–242.

193 H. Pan, W. Wang, Y. Pan, L. Song, Y. Hu and K. M. Liew, *Carbohydrate Polymers*, 2015, **115**, 516–524.

194 M. Hassan, M. Nour, Y. Abdelmonem, G. Makhlouf and A. Abdelkhalik, *Polymer Degradation and Stability*, 2016, **133**, 8–15.

195 B.-I. Andreica, X. Cheng and L. Marin, *European Polymer Journal*, 2020, **139**, 110016.

196 L. J. R. Foster, S. Ho, J. Hook, M. Basuki and H. Marçal, *PLOS ONE*, 2015, **10**, e0135153.

197 G. Cavallaro, G. Lazzara, S. Konnova, R. Fakhrullin and Y. Lvov, *Green Materials*, 2014, **2**, 232–242.

198 V. Bertolino, G. Cavallaro, G. Lazzara, S. Milioto and F. Parisi, *New Journal of Chemistry*, 2018, **42**, 8384–8390.

199 T. C. Yadav, P. Saxena, A. K. Srivastava, A. K. Singh, R. K. Yadav, Harish, R. Prasad and V. Pruthi, *Advanced Functional Textiles and Polymers*, Wiley, 2019, pp. 365–403.

200 M. Rubina, A. Shulenina, R. Svetogorov and A. Vasilkov, *Macromolecular Symposia*, 2020, **389**, 1900067.

201 R. Ying, H. Wang, R. Sun and K. Chen, *Materials Science and Engineering: C*, 2020, **110**, 110689.

202 X. Jia, I. Ahmad, R. Yang and C. Wang, *Journal of Materials Chemistry B*, 2017, **5**, 2459–2467.

203 A. B. Neji, M. Jridi, H. Kchaou, M. Nasri and R. Dhouib Sahnoun, *Polymer Testing*, 2020, **84**, 106380.

204 V. Bertolino, G. Cavallaro, G. Lazzara, M. Merli, S. Milioto, F. Parisi and L. Sciascia, *Industrial & Engineering Chemistry Research*, 2016, **55**, 7373–7380.

205 M. Liu, Y. Zhang, C. Wu, S. Xiong and C. Zhou, *International Journal of Biological Macromolecules*, 2012, **51**, 566–575.

206 L. Lisuzzo, G. Cavallaro, S. Milioto and G. Lazzara, *New Journal of Chemistry*, 2019, **43**, 10887–10893.

207 M. Liu, C. Wu, Y. Jiao, S. Xiong and C. Zhou, *Journal of Materials Chemistry B*, 2013, **1**, 2078.

208 I. Benucci, K. Liburdi, I. Cacciotti, C. Lombardelli, M. Zappino, F. Nanni and M. Esti, *Food Hydrocolloids*, 2018, **74**, 124–131.

209 X. Liu, S. Qin, H. Li, J. Sun, X. Gu, S. Zhang and J. C. Grunlan, *Macromolecular Materials and Engineering*, 2019, **304**, 1800531.

210 J. Prakash, D. Prema, K. Venkataprasanna, K. Balagangadharan, N. Selvamurugan and G. D. Venkatasubbu, *International Journal of Biological Macromolecules*, 2020, **154**, 62–71.

211 X. Li, Y.-C. Li, M. Chen, Q. Shi, R. Sun and X. Wang, *Journal of Materials Chemistry B*, 2018, **6**, 6544–6549.

212 Z.-K. Cui, S. Kim, J. J. Baljon, B. M. Wu, T. Aghaloo and M. Lee, *Nature Communications*, 2019, **10**, 3523.